ANTIOXIDANTS & REDOX SIGNALING
Volume 31, Number 18, 2019

DOI: 10.1089/ars.2019.7723

Discoveries

ORIGINAL RESEARCH COMMUNICATION

Salusin-β Promotes Vascular Calcification *via* Nicotinamide Adenine Dinucleotide Phosphate/Reactive Oxygen Species-Mediated Klotho Downregulation

Haijian Sun,[1,2,*] Feng Zhang,[1,*] Yu Xu,[1] Shuo Sun,[1] Huiping Wang,[2] Qiong Du,[2] Chenxin Gu,[3] Stephen M. Black,[4] Ying Han,[1] and Haiyang Tang[3,5]

Abstract

Aims: Vascular calcification (VC) is a hallmark feature of cardiovascular disease and a significant risk factor for morbidity and mortality. Salusin-β exerts cardiovascular regulating effects in hypertension, atherosclerosis, and diabetes. The present study was designed to examine the roles of salusin-β in the progression of VC and its downstream signaling mechanisms.

Results: Salusin-β expression in both the aortas of VC rats induced by vitamin D3 and nicotine and vascular smooth muscle cells (VSMCs) incubated with calcifying media was increased. Salusin-β knockdown remarkably reduced VC, whereas overexpression of salusin-β exacerbated VC both *in vitro* and *in vivo*. Overexpression of salusin-β promoted the VSMC osteochondrogenic transition, decreased Klotho protein levels, enhanced Ras-related C3 botulinum toxin substrate 1 (Rac1) activity and the translocation of p47phox to the membrane, increased the expression of nicotinamide adenine dinucleotide phosphate [NAD(P)H] oxidase subunits and the production of reactive oxygen species (ROS) with or without calcifying media; however, salusin-β deficiency played the opposite roles. The calcification and downregulated Klotho protein levels induced by salusin-β were restored by ROS scavenger N-acetyl-L-cysteine, diphenyleneiodonium chloride [an inhibitor of flavin-containing enzyme, including NAD(P)H oxidase], or gene knockdown of NAD(P)H oxidase (NOX)-2, p22phox, or p47phox but were not affected by NOX-1 and NOX-4 knockdown. Klotho knockdown attenuated the protective effect of salusin-β deficiency on VSMC calcification. By contrast, exogenous Klotho ameliorated the development of VC and ROS generation induced by salusin-β overexpression.

Innovation: Salusin-β is a critical modulator in VC.

Conclusion: Salusin-β regulates VC through activation of NAD(P)H/ROS-mediated Klotho downregulation, suggesting that salusin-β may be a novel target for treatment of VC. *Antioxid. Redox Signal.* 31, 1352–1370.

Keywords: vascular calcification, salusin, Klotho, ROS, NAD(P)H oxidase

[1]Key Laboratory of Targeted Intervention of Cardiovascular Disease, Collaborative Innovation Center of Translational Medicine for Cardiovascular Disease, Department of Physiology, Nanjing Medical University, Nanjing, China.
[2]Department of Basic Medicine, Wuxi School of Medicine, Jiangnan University, Wuxi, China.
[3]College of Veterinary Medicine, Northwest A&F University, Yangling, China.
[4]Division of Translational and Regenerative Medicine, College of Medicine, Department of Medicine, University of Arizona, Tucson, Arizona.
[5]State Key Laboratory of Respiratory Disease, National Clinical Research Center for Respiratory Disease, Guangzhou Institute of Respiratory Health, The First Affiliated Hospital of Guangzhou Medical University, Guangzhou, China.
*These authors contributed equally to this article.

Innovation

Vascular calcification (VC) is a critical feature of chronic kidney disease, diabetes, hypertension, and atherosclerosis, which is also a significant risk factor for cardiovascular morbidity and mortality. Salusin-β was a critical modulator in hypertension, atherosclerosis, and diabetes. Our results in this study innovatively highlight the essential role of salusin-β in the osteoblastic differentiation of vascular smooth muscle cells (VSMCs) and pathological arterial calcification. The downregulation of Klotho and excessive reactive oxygen species generation are driving factors for salusin-β to facilitate VC and osteochondrogenic transition of VSMCs. This study suggests that salusin-β is a potential therapeutic target for VC.

Introduction

Vascular calcification (VC) is a prevalent vascular pathophenotype that is highly associated with atherothrombotic cardiovascular diseases, diabetes mellitus, aging, and chronic kidney disease (57). It is also a well-recognized independent predictor for increased cardiovascular disease mortality (53). Vascular smooth muscle cells (VSMCs) are major cellular components of blood vessels and play a vital role in the regulation of vascular tension and blood pressure (19). Recent studies have demonstrated that VC is a highly active process of osteoblastic differentiation of VSMCs, much like bone formation (27). In the process of VC, VSMCs transforming into osteoblast-like cells is a core event (6). Under the pathological conditions such as oxidative stress, high phosphate levels, or high parathyroid hormone fragments, VSMCs undergo phenotypic changes that induce the expressions of mineralization regulating proteins such as alkaline phosphatase (ALP), osteopontin, and osteocalcin (38), which can be detected as indicators of the degree of VC. The complicated mechanisms underlying VC have yet to be fully elucidated; thus, the aim of this study was designed to identify novel regulatory factors in VC.

Salusins are characterized as two related peptides: salusin-α and salusin-β, with 28 and 20 amino acids, respectively (40). In contrast to salusin-α, salusin-β performs more cardiovascular regulation and accelerates the development of atherosclerosis (34). Compared with healthy controls, plasma salusin-β levels in patients with diabetes mellitus, coronary artery disease, and cerebrovascular disease are distinctly higher (8). It has been reported that salusin-β regulates blood pressure (36), activates sympathetic outflow (47), promotes the proliferation, migration, and foam cell formation of VSMCs (45, 48, 49), induces endothelial dysfunction (44), among additional roles. The dominance of salusin-β in VSMCs and fibroblasts was observed in human coronary atherosclerotic plaques (55). Furthermore, salusin-β increased intracellular concentration of Ca^{2+} in VSMCs of rats (40), thus providing a possibility that salusin-β is involved in the process of VC.

The pathogenesis of VC is multifactorial and complex and may involve oxidative stress due to its reported role as a critical regulator of arterial calcification (31). Oxidative stress can trigger bone morphogenetic protein 2/4 (BMP-2/4) signaling and matrix remodeling in the vasculature, which are crucial events in the development of VC (39). In light of oxidative stress, salusin-β is widely accepted as an oxidation inducer in cardiac tissues, VSMCs, and endothelial cells in multiple disease scenarios (44). The Klotho gene is a well-known anti-aging protein that protects cells from inflammation and oxidative stress (17). Klotho treatment protects the heart from hyperglycemia-induced injury by inactivating reactive oxygen species (ROS) signaling pathway (11). In particular, oxidative stress is an important regulator for Klotho gene expression, and the association of oxidative stress with Klotho plays a central role in the process of VC (32). It has been demonstrated that Klotho is a potential endogenous anticalcification factor (24). Although direct evidence linking salusin-β and Klotho is lacking, they might target the same oxidative stress signaling pathway. Based on this uncertainty, we sought to determine whether salusin-β was involved in the VC process and osteogenic differentiation of VSMCs both *in vitro* and *in vivo*, as well as to determine whether Klotho and ROS were implicated in salusin-β-mediated VC.

Results

Expressions of salusin-β in calcified VSMCs and aortas of rats

VC rats were induced by vitamin D3 combined with nicotine *in vivo*, and calcification of VSMCs of rats was induced by calcifying media containing of β-glycerophosphate (β-GP) with Ca^{2+} *in vitro*. During VSMC calcification, the messenger RNA (mRNA) and the level of salusin-β progressively increased compared with controls (Fig. 1A, B); this was also confirmed by immunofluorescent staining (Fig. 1E). Furthermore, we observed that the protein expression of salusin-β was upregulated in the calcified VSMCs (Fig. 1C, D), suggesting that calcification is a stimulator for salusin-β expression in VSMCs. Compared with control rats, salusin-β level in plasma of VC rats was increased (Fig. 1F), which was paralleled by increases in both protein level and mRNA expressions of salusin-β in the aortas of VC rats (Fig. 1G, H).

FIG. 1. The level of salusin-β in calcifying VSMCs and the aortas of rats. **(A)** Protein levels of salusin-β determined by ELISA, **(B)** mRNA levels of salusin-β, and **(C, D)** salusin-β protein expression in VSMCs stimulated by calcification medium at days 0, 3, 7, 10, and 14. Full blot is shown in Supplementary Figure S16. **(E)** Immunofluorescence staining of salusin-β in VSMCs at day 14 of stimulation. **(F)** Salusin-β levels in plasma, **(G)** mRNA level of salusin-β, and **(H)** protein level of salusin-β in the aortas of VC rats. **(I)** Immunohistochemistry staining of salusin-β in the aortas of VC rats. **(J)** Immunofluorescence double staining showed smooth muscle marker α-SMA (*green*) and salusin-β (*red*). Nuclei were stained by DAPI (*blue*). **(K)** Immunofluorescence double staining showed endothelial cell marker CD31 (*green*) and salusin-β (*red*). Nuclei were stained by DAPI (*blue*). Values are expressed as mean ± SE. $^{*}p < 0.05$ *versus* 0 day, $^{\dagger}p < 0.05$ *versus* Control. $n = 4$–6 for each group. α-SMA, alpha smooth muscle actin; ELISA, enzyme-linked immunosorbent assay; mRNA, messenger RNA; SE, standard error; VC, vascular calcification; VSMCs, vascular smooth muscle cells. Color images are available online.

Immunohistochemistry demonstrated the elevated salusin-β levels in the aortas of VC rats (Fig. 1I). Immunofluorescence double staining showed that salusin-β protein expression was markedly upregulated in the vascular media layer of VC rats (Fig. 1J), but not in the endothelium (Fig. 1K).

Roles of salusin-β in VSMC calcification

To investigate the potential role of salusin-β in VSMC calcification, adenoviral vectors encoding salusin-β small hairpin RNA (shRNA) or lentivirus expressing salusin-β were used in calcifying medium to knock down or overexpress salusin-β.

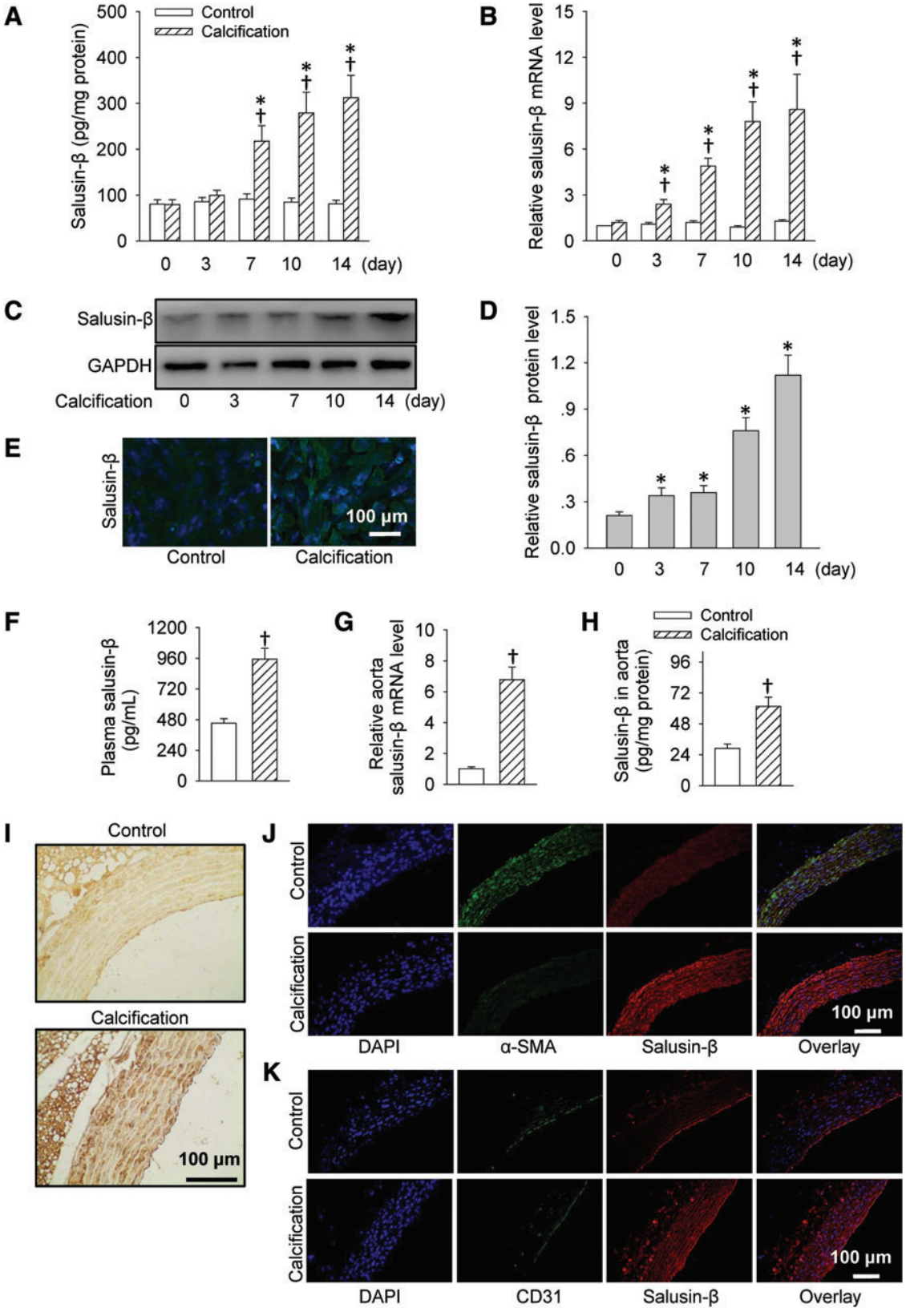

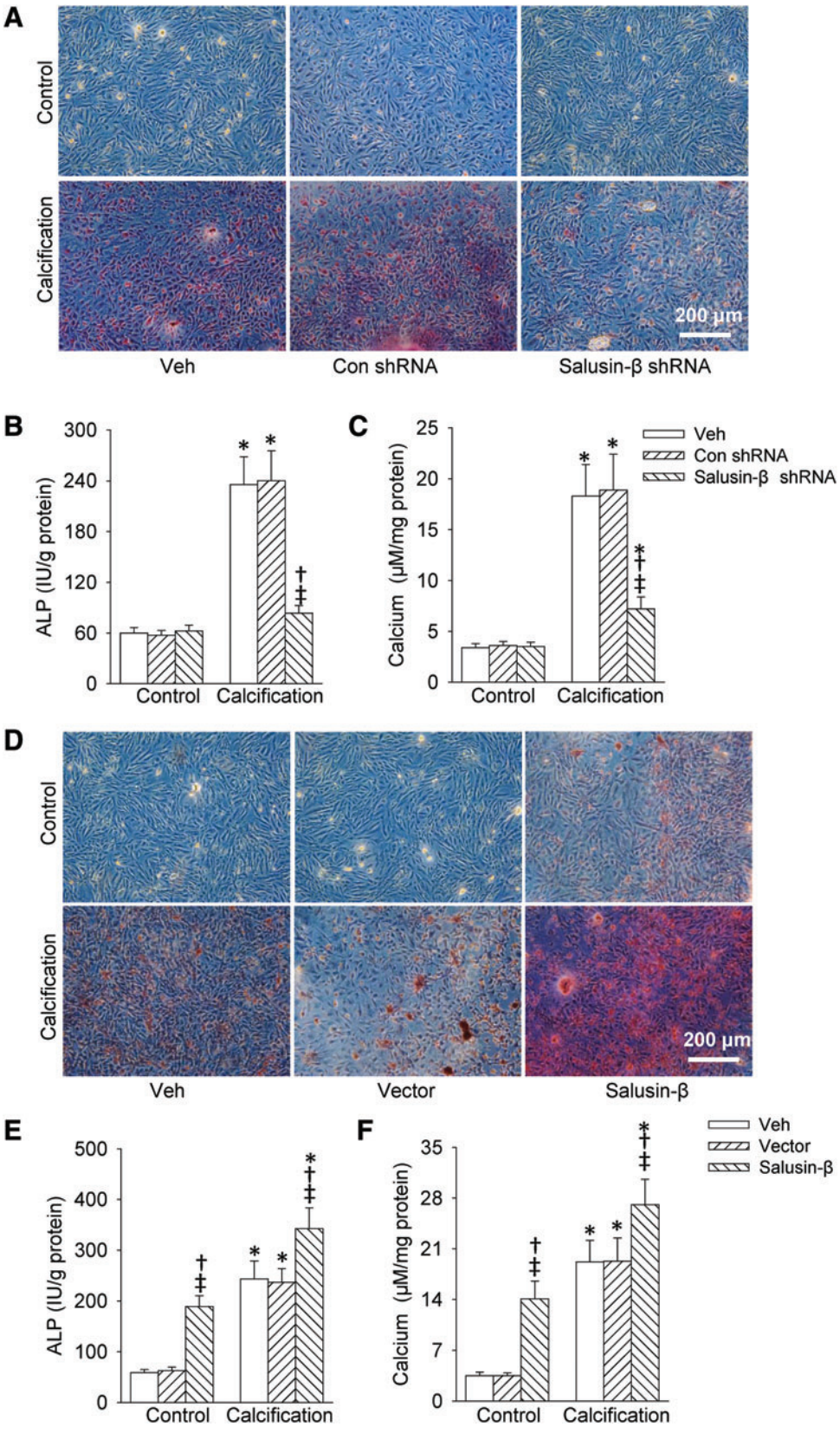

FIG. 2. Roles of salusin-β in VSMC calcification. **(A)** Alizarin-red S staining, **(B)** ALP activity, and **(C)** calcium content of calcified VSMCs after salusin-β knockdown. **(D)** Alizarin-red S staining, **(E)** ALP activity, and **(F)** calcium content of calcified VSMCs after salusin-β overexpression. Values are expressed as mean ± SE. $^{*}p < 0.05$ *versus* Control, $^{\dagger}p < 0.05$ *versus* Vehicle (Veh), $^{\ddagger}p < 0.05$ *versus* Control (Con) shRNA or Vector. $n = 4$–6 for each group. ALP, alkaline phosphatase; shRNA, small hairpin RNA. Color images are available online.

Specific knockdown or overexpression of salusin-β in VSMCs was verified at the mRNA and protein expressions (Supplementary Figs. S1 and S19). As expected, silencing of salusin-β alleviated calcium deposition in VSMCs, as evidenced from Alizarin Red S staining (Fig. 2A), ALP activity (Fig. 2B), and calcium content (Fig. 2C). Detected biochemically and histologically, overexpression of salusin-β not only greatly further exacerbated calcium deposition of calcified VSMCs compared with control cells but also induced spontaneous calcification even without calcifying stimulation (Fig. 2D–F).

Roles of salusin-β in VSMC phenotype switching

The phenotypic transition of VSMCs from a contractile phenotype to an osteogenic phenotype is a key event during pathological VC (6); therefore, we investigated the roles of salusin-β in VSMC phenotype switching. Incubation of VSMCs with calcification medium remarkably reduced the expression of contractile markers, including alpha smooth muscle actin (α-SMA) and smooth muscle 22 alpha (SM22α) but enhanced the expression of osteogenic switching markers, including runt-related transcription factor 2 (Runx2) and BMP-2 of VSMCs. These phenotypic changes were antagonized by salusin-β shRNA treatment (Fig. 3A, B), but further deteriorated by ectopic overexpression of salusin-β (Fig. 3C, D). Additionally, salusin-β overexpression led to spontaneous osteogenic conversion of VSMCs (Fig. 3C, D).

Effects of salusin-β on Klotho levels in calcified VSMCs

Previous studies revealed that Klotho attenuates VC, and overexpression of Klotho suppresses calcification in VSMCs (16, 24). We sought to investigate whether Klotho signaling was involved in salusin-β-mediated VC. The Klotho protein level showed a persistent decline in calcified VSMCs during the 14 days of calcified medium stimulation (Fig. 4A). Alizarin Red S staining (Fig. 4B), ALP activity results (Fig. 4C), and calcium content assay (Fig. 4D) showed that treatment with exogenous Klotho dramatically diminished calcium deposition in calcified medium-incubated VSMCs, suggesting that Klotho antagonizes VSMC calcification. The reduced Klotho protein (Fig. 4E) and mRNA levels (Supplementary Fig. S2A) in calcified VSMCs were restored by salusin-β silencing but was intensified in salusin-β-overexpressed VSMCs (Fig. 4F and Supplementary Fig. S2B). Interestingly, gene knockdown of salusin-β had no effect on the mRNA and protein levels of Klotho without calcified stimulation, whereas overexpression of salusin-β alone in VSMCs also remarkably decreased Klotho protein and mRNA levels (Fig. 4E, F, and Supplementary Fig. S2A, B). To further investigate the role of Klotho in salusin-β-mediated VC, we knocked down Klotho using small interfering RNA (siRNA). In cultured VSMCs, the protein expression of Klotho was substantially reduced by Klotho-targeting siRNA (Supplementary Fig. S3). In calcified VSMCs, the increased calcium content and ALP activity were significantly inhibited by silencing of salusin-β, but these protective effects were diminished by Klotho-targeting siRNA (Fig. 4G–I).

Effects of salusin-β on oxidative stress in calcified VSMCs

It is known that oxidative stress is a requisite event in the shift to osteoblastic behavior and calcification of VSMCs (4). We investigated whether ROS were involved in salusin-β-mediated VC. Protein levels of the nicotinamide adenine

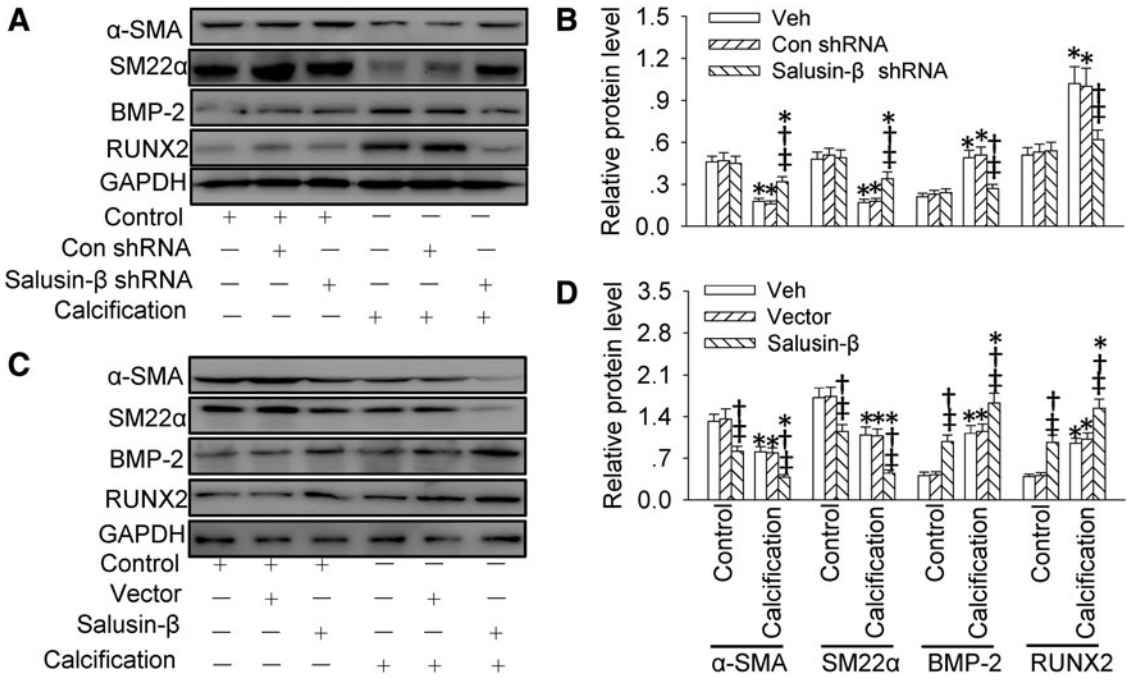

FIG. 3. Roles of salusin-β in VSMC phenotype switching. (A, B) Contractile markers α-SMA and SM22α and osteogenic switching markers BMP-2 and Runx2 proteins expression of VSMCs after salusin-β knockdown. Full blot is shown in Supplementary Figure S16. **(C, D)** α-SMA, SM22α, BMP-2, and Runx2 proteins expression of VSMCs after salusin-β overexpression. Full blot is shown in Supplementary Figure S16. Values are expressed as mean ± SE. $^{*}p<0.05$ *versus* Control, $^{\dagger}p<0.05$ *versus* Veh, $^{\ddagger}p<0.05$ *versus* Control (Con) shRNA or Vector. $n=4$ for each group. BMP-2, bone morphogenetic protein 2; Runx2, runt-related transcription factor 2; SM22α, smooth muscle 22 alpha.

dinucleotide phosphate [NAD(P)H] oxidase subunits $p22^{phox}$, $p47^{phox}$, and NAD(P)H oxidase (NOX)-2 in VSMCs were upregulated gradually across the calcification induction process (Fig. 5A). In line with expressions of NOX-2, $p22^{phox}$, and $p47^{phox}$, fluorescence staining also showed that ROS levels were progressively increased from day 0 to day 14 (Fig. 5B, C). Malondialdehyde (MDA), a well-studied marker of lipid peroxidation, and hydrogen peroxide (H_2O_2) are proposed as biological markers of oxidative stress in cardiovascular disease (14). The levels of MDA and H_2O_2

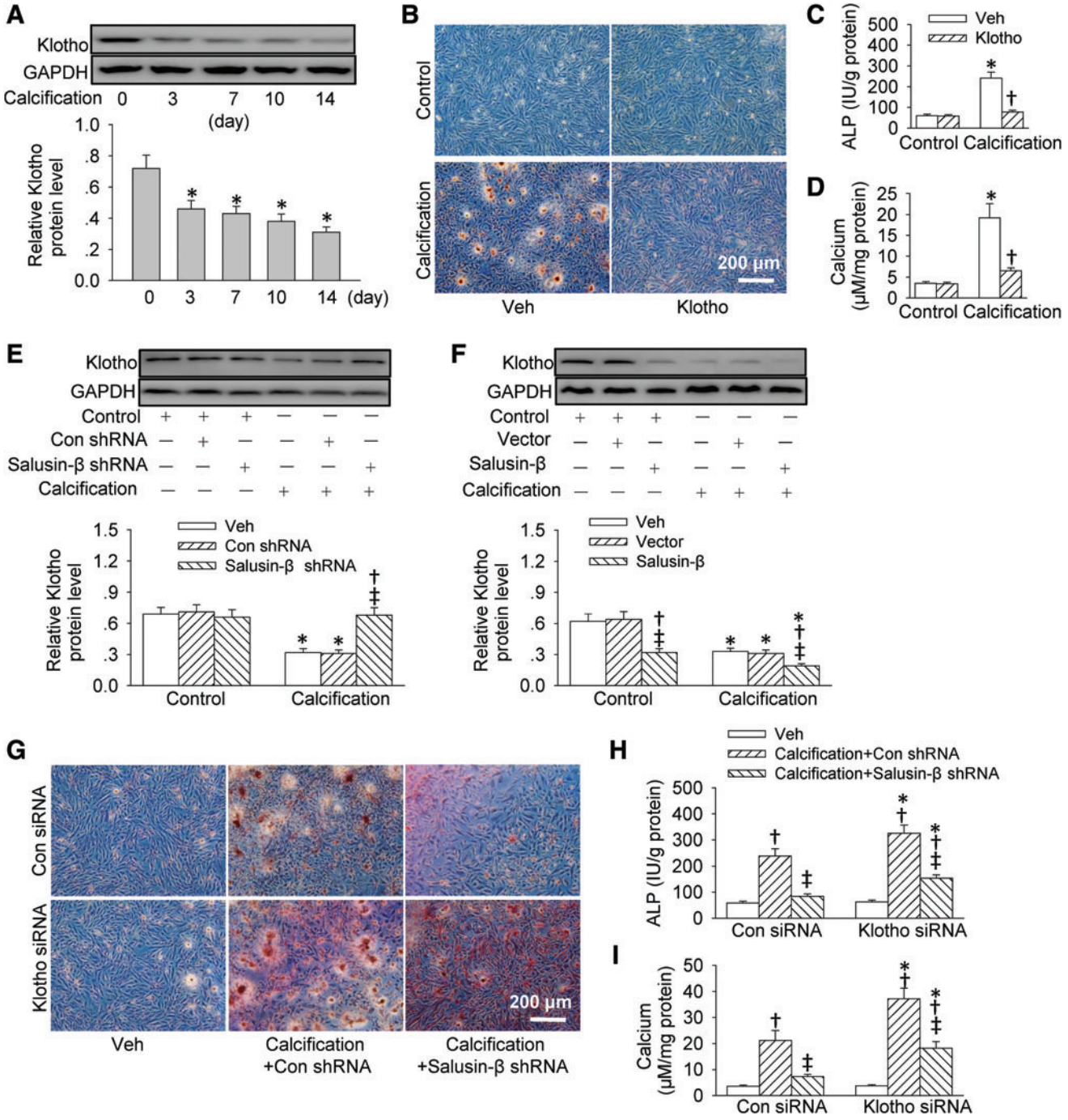

FIG. 4. Effects of salusin-β on Klotho protein level in calcifying VSMCs. **(A)** Klotho protein level of VSMCs during VC induction by calcification medium at days 0, 3, 7, 10, and 14. Full blot is shown in Supplementary Figure S17. **(B)** Alizarin-red S staining, **(C)** ALP activity, and **(D)** calcium content of VSMCs pretreated with Klotho (0.4 μg/mL) for 6 h followed by stimulation with calcification medium. **(E)** Klotho protein level of calcifying VSMCs after salusin-β knockdown. Full blot is shown in Supplementary Figure S17. **(F)** Klotho protein level of calcifying VSMCs after salusin-β overexpression. Full blot is shown in Supplementary Figure S17. **(G)** Alizarin-red S staining, **(H)** ALP activity, and **(I)** calcium content of calcifying VSMCs transfected with Klotho siRNA (100 n*M*) with or without salusin-β knockdown. Values are expressed as mean ± SE. $^{*}p < 0.05$ *versus* 0 day or Control or Control (Con) siRNA, $^{\dagger}p < 0.05$ *versus* Veh, $^{\ddagger}p < 0.05$ *versus* Con shRNA, Vector, or Calcification+Con shRNA. $n = 4$–6 for each group. siRNA, small interfering RNA. Color images are available online.

content were markedly enhanced in VSMCs after calcification induction (Fig. 5D, E). Next, we investigated if the blockade of NAD(P)H oxidase-derived ROS ameliorated the development of VC. Pretreating VSMCs with diphenyleneiodonium chloride [DPI, an inhibitor of flavin-containing enzyme, including NAD(P)H oxidase] or N-acetyl-L-cysteine, (NAC, an ROS scavenger) enormously reduced ROS production in a calcification environment, as observed by dihydroethidium (DHE) staining, MDA content, and H_2O_2 formation (Supplementary Fig. S4A–D). Furthermore, treatment with both DPI and NAC blocked the calcified medium-induced VSMC calcification (Fig. 5F–H).

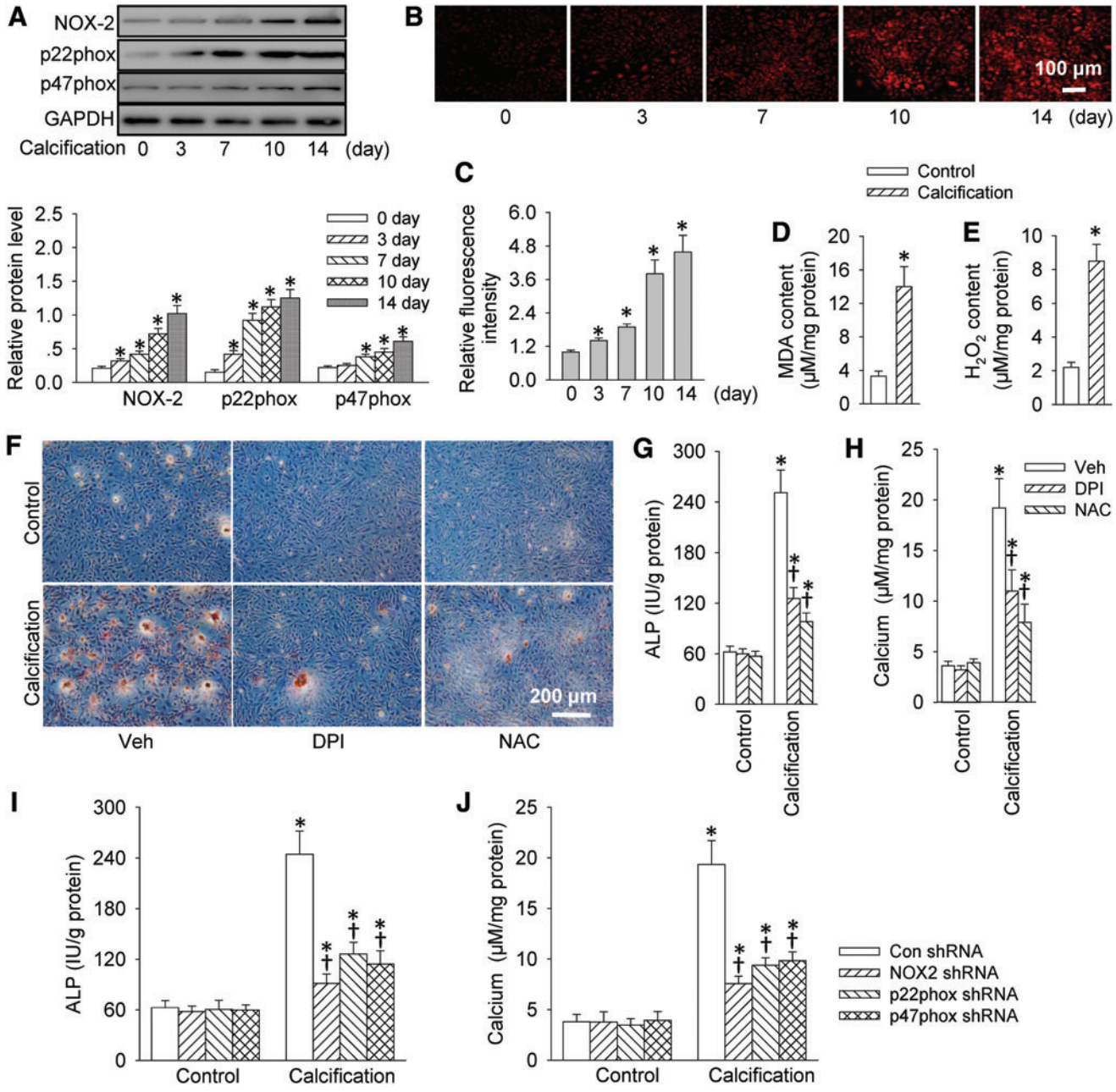

FIG. 5. Roles of NAD(P)H oxidase-derived ROS in VC. (A) Expression of the $p22^{phox}$, $p47^{phox}$, and NOX-2 proteins of VSMCs during stimulation by calcification medium for 0, 3, 7, 10, and 14 days. Full blot is shown in Supplementary Figure S17. **(B, C)** ROS levels in calcifying VSMCs detected by DHE staining, **(D)** MDA content, and **(E)** H_2O_2 levels. **(F)** Alizarin-red S staining, **(G)** ALP activity, and **(H)** calcium content of VSMCs that were pretreated with NAC (1 m*M*) or DPI (10 μM) for 30 min and then challenged with calcification medium. **(I)** The ALP activity and **(J)** calcium content in VSMCs responses to calcification medium after $p22^{phox}$, $p47^{phox}$, and NOX-2 knockdown. Values are expressed as mean ± SE. $^*p < 0.05$ *versus* 0 day or Control, $^{\dagger}p < 0.05$ *versus* Veh or Control (Con) shRNA. $n = 4$–6 for each group. DHE, dihydroethidium; DPI, diphenyleneiodonium chloride; H_2O_2, hydrogen peroxide; MDA, malondialdehyde; NAC, N-acetyl-L-cysteine; NAD(P)H, nicotinamide adenine dinucleotide phosphate; NOX, NAD(P)H oxidase; ROS, reactive oxygen species. Color images are available online.

To investigate the exact role of NAD(P)H oxidase subunits in the VC, VSMCs were transfected with shRNA targeting NOX-2, $p22^{phox}$, or $p47^{phox}$ to knockdown these NAD(P)H oxidase subunits. The interference effectiveness of the shRNAs was ascertained by the downregulations of targeted protein expressions (Supplementary Fig. S5). As expected, gene deficiency of NOX-2, $p22^{phox}$, or $p47^{phox}$ impeded VSMC calcification induced by calcification medium, as evidenced by reduced ALP activity and calcium content (Fig. 5I, J). These results confirmed the critical role of NAD(P)H oxidases-derived ROS in VSMC calcification.

The upregulated NAD(P)H oxidase subunits $p22^{phox}$, $p47^{phox}$, and NOX-2 protein levels in calcified VSMCs were obstructed by deficiency of salusin-β (Fig. 6A, B) but were further raised by salusin-β overexpression (Fig. 6C, D). Moreover, salusin-β overexpression independent of calcified medium increased $p22^{phox}$, $p47^{phox}$, and NOX-2 protein levels (Fig. 6C, D) and ROS generation (Supplementary

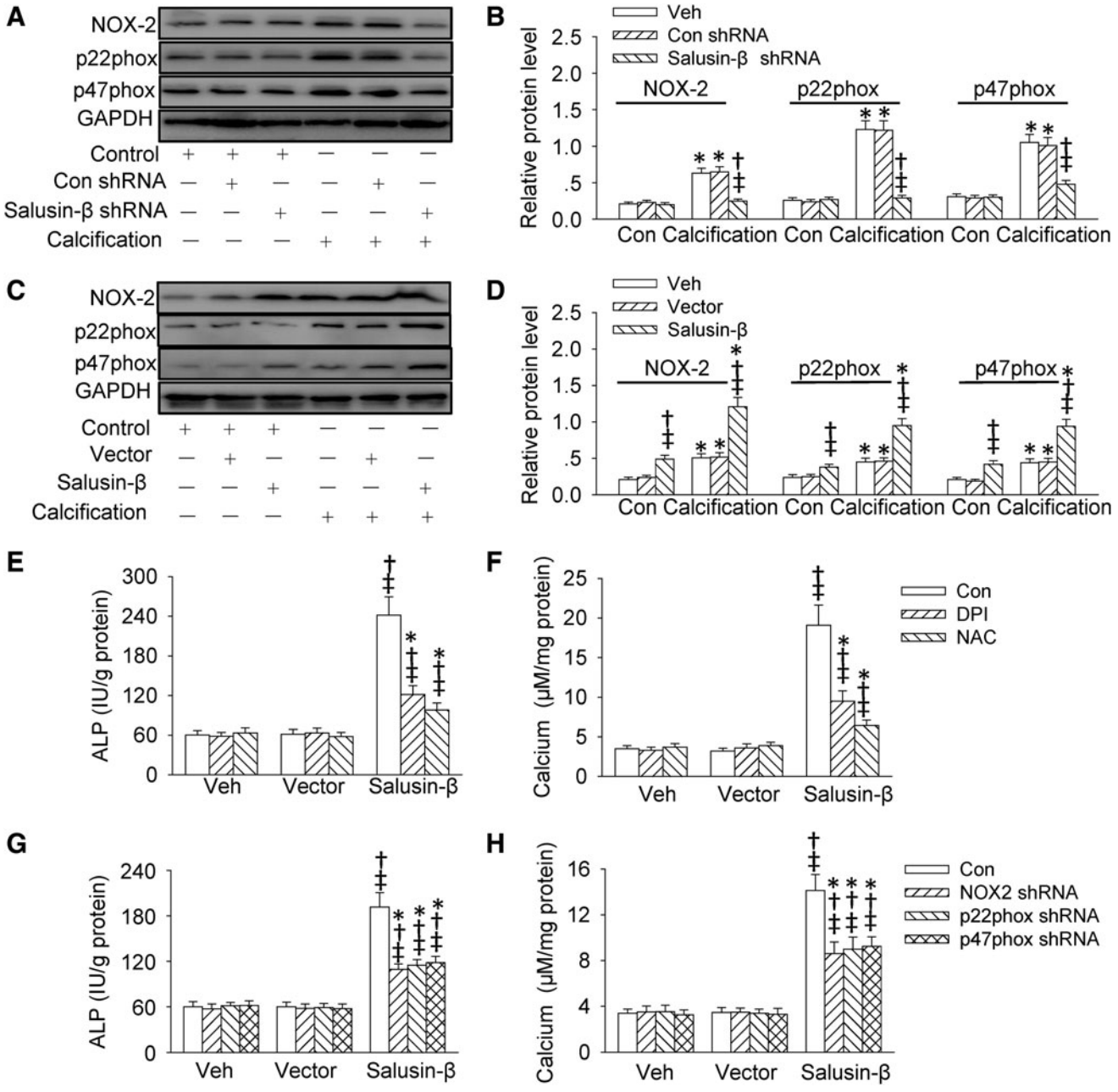

FIG. 6. Effects of salusin-β on oxidative stress in calcifying VSMCs. (A, B) Protein levels of the $p22^{phox}$, $p47^{phox}$, and NOX-2 of calcifying VSMCs after salusin-β knockdown. Full blot is shown in Supplementary Figure S17. **(C, D)** Protein levels of $p22^{phox}$, $p47^{phox}$, and NOX-2 of calcifying VSMCs after salusin-β overexpression. Full blot is shown in Supplementary Figure S17. **(E)** The ALP activity and **(F)** calcium content in VSMCs pretreated with NAC (1 m*M*) or DPI (10 μM) 30 min before salusin-β overexpression. **(G)** The ALP activity and **(H)** calcium content in VSMCs responses to salusin-β overexpression after $p22^{phox}$, $p47^{phox}$, and NOX-2 knockdown. Values are expressed as mean ± SE. $^{*}p < 0.05$ *versus* Control (Con), $^{\dagger}p < 0.05$ *versus* Veh, $^{\ddagger}p < 0.05$ *versus* Con shRNA or Vector. $n = 4$–6 for each group.

Fig. S4E–H) of VSMCs directly. Consistently, salusin-β-induced ROS generation was almost abolished by NAC and DPI (Supplementary Fig. S4E–H). Furthermore, NAC and DPI relieved both aberrant ALP activity (Fig. 6E) and calcium content (Fig. 6F) induced by salusin-β overexpression. Elevated ALP activity and calcium content in salusin-β-overexpressed VSMCs were dramatically normalized by gene deletion of NOX-2, $p22^{phox}$, or $p47^{phox}$ (Fig. 6G, H), suggesting that NAD(P)H oxidase subtypes and derived ROS were involved in salusin-β-mediated VC.

Activation of NOX-2 requires the translocation of $p47^{phox}$ from the cytosol to the membrane (2). We found that after stimulating VSMCs with calcification medium, $p47^{phox}$ was observed to translocate from the cytosol to the membrane, as manifested by increased membrane $p47^{phox}$ expression and decreased cytoplasmic $p47^{phox}$ (Supplementary Fig. S6). As expected, silencing of salusin-β in VSMCs (Supplementary Fig. S6A, B) blocked the translocation of $p47^{phox}$, whereas overexpression of salusin-β (Supplementary Fig. S6C, D) enhanced the translocation of $p47^{phox}$ to the membrane under the calcification medium.

Ras-related C3 botulinum toxin substrate 1 (Rac1, a small GTPase protein) is an important subunit of NAD(P)H oxidase that is required for the assembly and activation of NAD(P)H oxidase and the production of ROS (1). However, whether Rac1 is involved in salusin-β-elicited NAD(P)H oxidase activation and ROS production has not yet been fully elucidated. We found that treatment of VSMCs with the Rac1 peptide inhibitor W56 remarkably relieved the increased ALP activity and calcium content in calcified medium-incubated VSMCs (Supplementary Figs. S7A, B and S20). Importantly enough, the active form of Rac1, Rac1-GTP, was obviously upregulated in VSMCs induced by calcified medium, whereas salusin-β silencing markedly reduced the Rac1-GTP level (Supplementary Fig. S7C). Conversely, the level of Rac1-GTP was elevated in VSMCs with salusin-β overexpression (Supplementary Fig. S7D).

The NOX family of NAD(P)H oxidases is composed of five members (NOX1 to NOX5) and the Duox family contains two (Duox1 and Duox2), which are believed to be responsible for ROS production in diverse tissues (9). NOX-1, NOX-2, and NOX-4 are observed in VSMCs, with NOX-1 and NOX-4 being the most abundant (13, 21). Besides NOX-2, we also observed whether NOX-1 and NOX-4 were involved in the effect of salusin-β on oxidative stress in calcified VSMCs. In parallel to NOX-2, calcification medium increased expression levels of both NOX-1 and NOX-4 in VSMCs (Supplementary Fig. S8A) in a time-dependent manner. When compared with control shRNA, the protein levels of NOX-1 or NOX-4 were largely reduced by their targeted shRNAs (Supplementary Fig. S8B). Not surprisingly, silencing of either NOX-1 or NOX-4 prevented the increased ALP activity and calcium deposition in VSMCs upon exposure of calcification medium (Supplementary Fig. S8C, D). However, the salusin-β-triggered VSMC calcification was not altered by knockdown of NOX-1 and NOX-4 (Supplementary Fig. S8E, F). In accordance with this, neither salusin-β knockdown nor salusin-β overexpression affected the expressions of NOX-1 and NOX-4 in the absence or presence of calcification stimulants (Supplementary Fig. S8G, H). These results suggest that NOX-1 and NOX-4 are crucial players in VSMC calcification, whereas neither is required for salusin-β-mediated oxidative stress in VSMCs.

Interplay of oxidative stress and Klotho responses to salusin-β

It has been reported that oxidative stress is an important regulator for Klotho gene expression, and the link between oxidative stress and Klotho plays a central role in the process of VC (32). We wanted to determine the mechanisms of ROS and Klotho in the downstream signaling pathway of salusin-β in respect to VC. Both DPI (Fig. 7A) and NAC (Fig. 7B) were able to rescue the downregulated Klotho protein expression in calcified medium-incubated VSMCs. Additionally, the reduced Klotho protein levels in VSMCs post-salusin-β challenge were also reversed by DPI (Fig. 7C) and NAC (Fig. 7D). Similarly, deficiency of NOX-2 was also capable of restoring the decreased protein level of Klotho in either calcified medium-challenged VSMCs (Fig. 7E) or salusin-β-overexpressing VSMCs (Fig. 7F), further confirming the involvement of NOX-2 in the regulation of Klotho level responses to calcified stimulation or salusin-β. Furthermore, salusin-β protein expression in the VSMCs was not affected by the pretreatment with DPI and NAC with or without calcification medium (Supplementary Fig. S9). These results suggested that ROS was responsible for salusin-β-mediated Klotho downregulation, but not for the upregulation of salusin-β in the calcified medium-incubated VSMCs.

It appears that the Klotho gene might exhibit antioxidant properties (32, 35). Therefore, we investigated whether salusin-β-elicited oxidative stress can be altered by the addition of Klotho. We found that administration of exogenous Klotho prevented the overproduction of superoxide anions, MDA, and H_2O_2 induced by calcified medium (Supplementary Fig. S10A–C). In agreement with these findings, the excessive oxidative stress in VSMCs with salusin-β overexpression was dampened by the treatment of Klotho (Supplementary Fig. S10D–F).

Roles of salusin-β on VC in rat aortas

To further investigate the potential role of salusin-β in arterial calcification, rats were given intravenous injection of adenoviral vectors encoding salusin-β shRNA or lentivirus vector expressing salusin-β to either knock down or overexpress salusin-β, respectively. Real-time polymerase chain reaction (PCR) results demonstrated increased mRNA levels of salusin-β in calcified aortas of rats, which were blocked by salusin-β shRNA (Supplementary Fig. S11A), but further elevated by overexpression of salusin-β (Supplementary Fig. S11B). Von Kossa staining showed that salusin-β knockdown decreased calcium-phosphate salt deposition (Fig. 8A), as well as reduced the ALP activity and calcium content in the aortas of VC rats (Fig. 8B, C). Conversely, the overexpression of salusin-β led to increased calcium phosphate salt deposition (Fig. 8D), ALP activity (Fig. 8E), and calcium content (Fig. 8F) in both control and calcified aortas.

Effect of salusin-β on NAD(P)H/ROS/Klotho signaling in the aortas of VC rats

Compared with control rats, VC rats demonstrated higher expression levels of NAD(P)H oxidase subunits $p22^{phox}$, $p47^{phox}$, and NOX-2, but lower Klotho protein expression in the aortas, which were significantly circumvented by salusin-β deficiency (Fig. 9A, C). Interestingly, salusin-β overexpression aggravated the abnormal expressions of

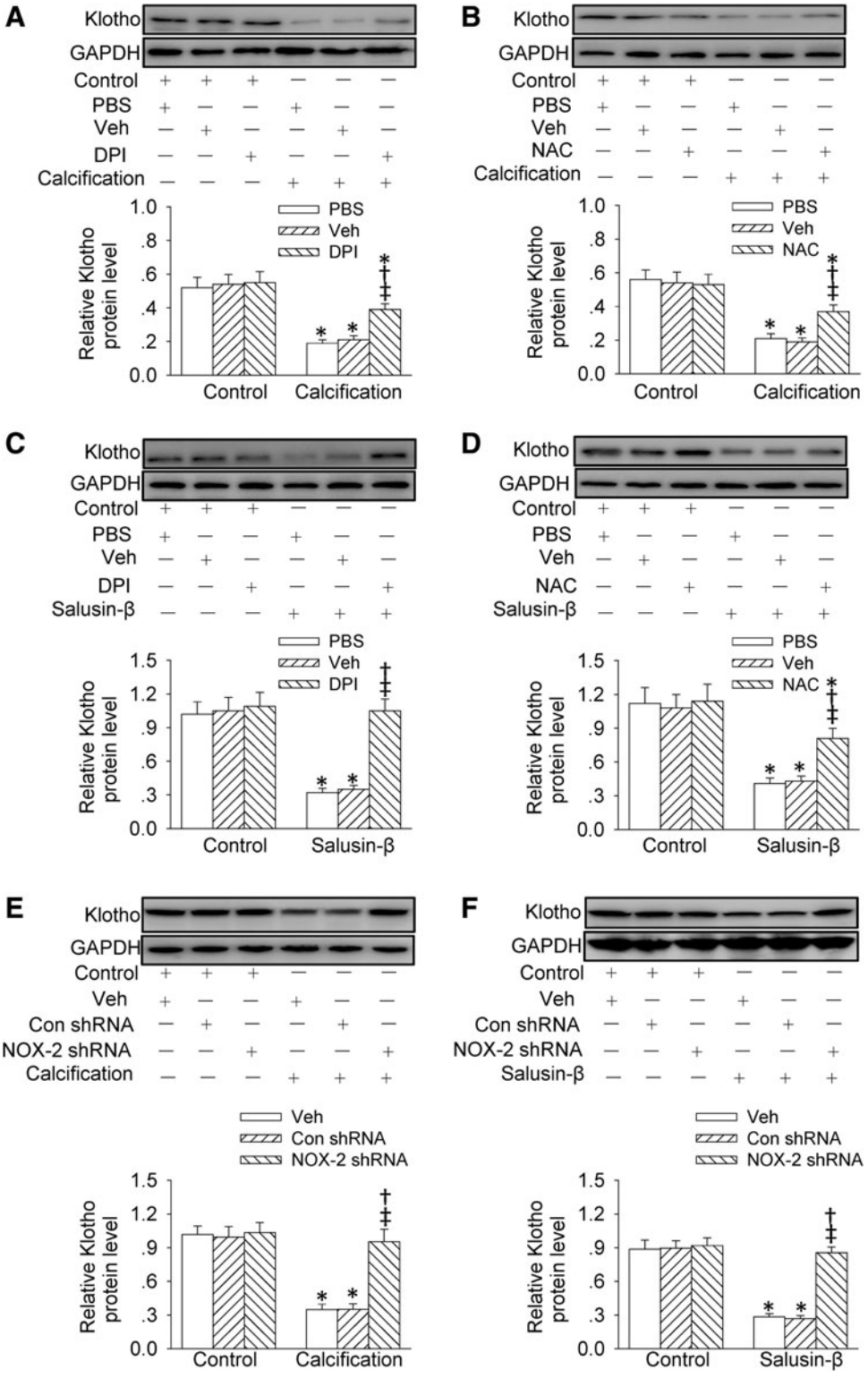

FIG. 7. Effects of oxidative stress on Klotho downregulation. (A, B) Klotho protein levels of VSMCs that were pretreated with DPI (10 μM) or NAC (1 mM) for 30 min before calcification medium stimulation. **(C, D)** Klotho protein levels of VSMCs pretreated with DPI or NAC before salusin-β overexpression. **(E)** Klotho protein levels of VSMCs pretreated with NOX-2 shRNA before calcification medium stimulation. **(F)** Klotho protein levels of VSMCs pretreated with NOX-2 shRNA before salusin-β overexpression. Full blot is shown in Supplementary Figure S18. Values are expressed as mean ± SE. $^{*}p < 0.05$ *versus* Control, $^{\dagger}p < 0.05$ *versus* PBS, $^{\ddagger}p < 0.05$ *versus* Veh. $n = 4$ for each group. PBS, phosphate-buffered solution.

NAD(P)H oxidase subunits $p22^{phox}$, $p47^{phox}$, and NOX-2 as well as Klotho in calcified aortas (Fig. 9B, D). Moreover, knockdown of salusin-β (Fig. 9E, F) eradicated, whereas overexpression of salusin-β (Fig. 9G, H) intensified the overproduction of MDA and H_2O_2 in calcified aortas.

Because the importance of Klotho in salusin-β-induced VC changes is currently unknown, we explored whether Klotho overexpression could reverse salusin-β-induced VC and ROS in the aortas of rats *in vivo*. After tail vein injection of lentivirus expressing salusin-β, rats underwent intraperitoneal injection of Klotho at 0.01 g/kg per 48 h for 4 weeks as described in previous report (26). As expected, the effects of salusin-β overexpression on the development of VC and NAD(P)H oxidase-derived ROS production of aortas were largely ameliorated by chronic application of Klotho, indicated by the ALP activity and calcium content

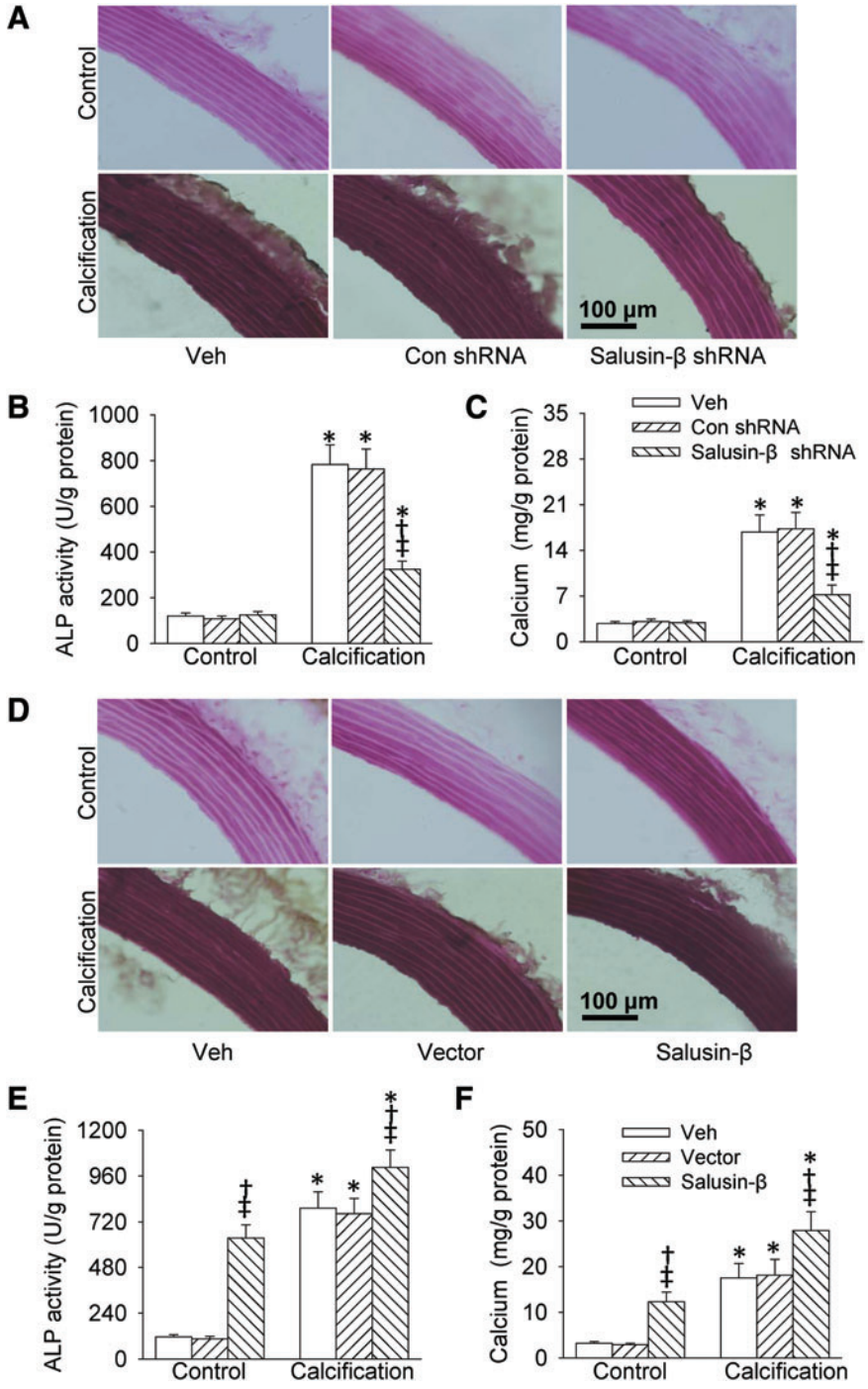

FIG. 8. Roles of salusin-β in the calcification of the aortas in rats. (A–C) The von Kossa staining, ALP activity, and calcium content of the aortas of rats after salusin-β knockdown. **(D–F)** The von Kossa staining, ALP activity, and calcium content of the aortas of rats after salusin-β overexpression. Values are expressed as mean ± SE. $^{*}p < 0.05$ *versus* Control, $^{\dagger}p < 0.05$ *versus* Veh, $^{\ddagger}p < 0.05$ *versus* Control (Con) shRNA or Vector. $n = 4$–6 for each group. Color images are available online.

(Supplementary Fig. S12A, B), and NAD(P)H oxidase activity and ROS level (Supplementary Fig. S12C, D).

Discussion

VC is established as a complex and active process, rather than an inevitable, passive, and degenerative course (18). To date, substantive research has demonstrated that high calcium phosphate products, oxidative stress, BMPs, cell apoptosis, and inflammation are all critical contributors to osteochondrogenic transition of VSMCs and VC (54). However, the molecular and cellular mechanisms of VC are still not fully elucidated. Our study demonstrates that salusin-β may act as a novel endogenous inducer of VC through oxidative stress-mediated Klotho suppression. These findings suggest that intervention of salusin-β may be a therapeutic strategy for managing VC.

VC rats induced by vitamin D3 combined with nicotine *in vivo* and calcification of VSMCs induced by combination of β-GP with Ca^{2+} *in vitro* have been taken as classical models of VC (30). The degree of VC can be assessed by increased ALP activity, calcium deposition, and pathological changes. In this study, we found that salusin-β levels were upregulated in both the aortas of VC rats and cultured VSMCs exposed to calcification medium stimulation. Dysregulated ALP activity, calcium deposition, and pathological changes in calcified aortic tissues and VSMCs were rescued

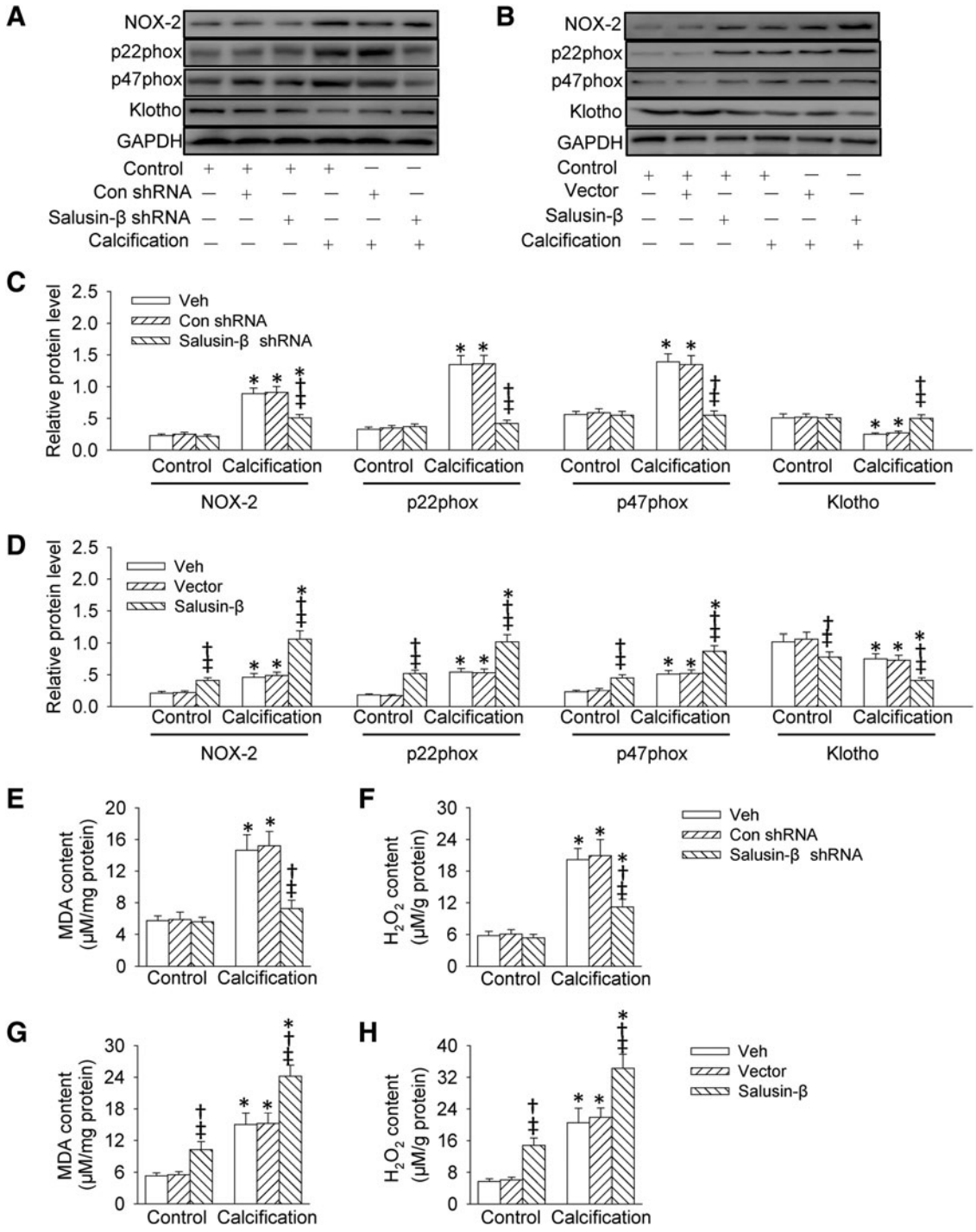

FIG. 9. Effects of salusin-β on oxidative stress and Klotho protein expression of the aortas of VC rats. (A, C) Protein levels of the $p22^{phox}$, $p47^{phox}$, NOX-2, and Klotho of the aortas in rats with salusin-β knockdown. Full blot is shown in Supplementary Figure S18. **(B, D)** Protein levels of the $p22^{phox}$, $p47^{phox}$, NOX-2, and Klotho of the aortas in rats with salusin-β overexpression. Full blot is shown in Supplementary Figure S18. **(E, F)** MDA and H_2O_2 levels of the aortas in response to salusin-β knockdown. **(G, H)** MDA and H_2O_2 levels of the aortas in response to salusin-β overexpression. Values are expressed as mean ± SE. $^*p < 0.05$ *versus* Control, $^\dagger p < 0.05$ *versus* Veh, $^\ddagger p < 0.05$ *versus* Control (Con) shRNA or Vector. $n = 4$–6 for each group.

by salusin-β knockdown but exacerbated by overexpression of salusin-β. Both *in vivo* and *in vitro* studies verified that the salusin-β gene played critical roles in the development of VC. Notably, salusin-β overexpression stimulated calcium deposition and ALP activity in aortic tissues *in vivo* and in VSMCs *in vitro* even in the absence of a calcifying environment. This suggests that calcification-prone conditions are not necessary for the direct action of salusin-β on VC, rather, salusin-β can induce VC directly. Future studies will investigate the abnormal expression of salusin-β in some conditions such as oxidative stress, cell apoptosis, and inflammation as a key event in the induction of VC.

Unlike most cell types with terminal differentiation characteristics, VSMCs retain substantial phenotypic plasticity, even in response to detrimental stimuli, including calcification environment (51). VC is also reflected by osteochondrogenic differentiation markers, including Runx2 and BMP-2, and inhibition of smooth muscle cell lineage markers α-SMA and SM22α (5). Our results showed that the protein levels of contractile phenotype markers (SM22α and α-SMA) were significantly lower, but osteoblast-like phenotype markers (Runx2 and BMP-2) were significantly higher in calcifying VSMCs, which is a critical step for VSMC transformation from a contractile phenotype into an osteoblast-like phenotype, as well as calcification (7). We additionally found that salusin-β knockdown inhibited gene expressions responsible for the osteoblast-like transformation of VSMCs, whereas overexpression of salusin-β had the reverse effect. These results suggest that salusin-β is responsible for VC associated with osteoblast-like differentiation of VSMCs.

A growing body of evidence has shown that mice lacking Klotho (an endogenous anticalcification factor) develop VC, whereas Klotho transgenic mice exhibit less calcification compared with wild-type mice with chronic kidney disease (16, 24). Klotho protein is downregulated in the early stage of chronic kidney disease (41) and acts as a circulating or resident protein, playing a protective role in vascular pathology including VC (15). Restoration of native vascular Klotho expression is suggested as a therapeutic objective for the prevention or treatment of VC (24). The existing evidence drove us to explore whether Klotho signaling was implicated in salusin-β-mediated VC. Our results showed that the protein expression of Klotho was decreased in calcified VSMCs and aortas, and Klotho pretreatment suppressed VSMC calcification. The downregulated Klotho protein expression induced by calcification was reversed by salusin-β shRNA but was further decreased by salusin-β overexpression *in vivo* and *in vitro*, suggesting that Klotho may be a targeted gene of salusin-β. More importantly, the protective effect of salusin-β knockdown on VC was attenuated by Klotho siRNA. These results imply that salusin-β reduces Klotho protein levels to trigger calcification. We also found that the Klotho mRNA level in calcified VSMCs was also reduced and restored by salusin-β silence, but the reduction was intensified in salusin-β-overexpressed VSMCs. Furthermore, overexpression of salusin-β alone in VSMCs directly decreased Klotho both protein and mRNA levels. These results indicated that salusin-β might induce Klotho protein downregulation through inhibiting its gene expression. In addition, chronic application of exogenous Klotho largely mitigated that salusin-β overexpression induced the development of VC in the aortas of rats, which suggest that Klotho has the ability to fight with salusin-β to play the anticalcification role.

It is known that oxidative stress is a major driver of calcification in atherosclerosis and chronic kidney disease (12). Some studies have suggested that the role of oxidative stress in VC deserves careful consideration, since it may be a target for the treatment of VC (4). Advanced glycation end products have been shown to promote the phenotypic switch of VSMCs to osteoblast-like cells and VC through the activation of NAD(P)H oxidase-derived ROS production (20). NAD(P)H is a cofactor required to reduce glutathione and promote ROS production (10), and the subunits of NOX-2, $p22^{phox}$, and $p47^{phox}$ are major sources of ROS in the vascular wall (44). In this study, VSMC calcification was prevented by either NAC (a ROS scavenger) or DPI [an inhibitor of flavin-containing enzyme, including NAD(P)H oxidase], indicating that oxidative stress is a major mediator in VSMC calcification. We also found that expressions of NAD(P)H oxidase subunits (including NOX-2, $p22^{phox}$, and $p47^{phox}$) and ROS generation were increased in both calcified VSMCs and aortas; this was suppressed by shRNA-mediated salusin-β silencing but was enhanced by overexpression of salusin-β. In addition, overexpression of salusin-β alone in VSMCs directly increased NOX-2, $p22^{phox}$, and $p47^{phox}$ expressions and ROS generation. Administration of either NAC or DPI attenuated the salusin-β-induced increases of ALP activity and calcium deposition in VSMCs. Gene knockdown of NOX-2, $p22^{phox}$, or $p47^{phox}$ obviously impeded calcification medium or salusin-β overexpression-induced VSMC calcification. These results suggested that NAD(P)H oxidase-derived ROS mediated the effect of salusin-β on calcification, and the subunits of NAD(P)H oxidase (NOX-2, $p22^{phox}$, and $p47^{phox}$) were involved.

It has been reported that the translocation of $p47^{phox}$ from cytosol to the membrane is required for the activation of NOX-2 (2), and the activity of NOX-2 is positively associated with the membrane translocation level of $p47^{phox}$ (56). In this study, we found that the translocation of $p47^{phox}$ from cytosol to the membrane of VSMCs increased under calcification medium stimulation, and silencing of salusin-β inhibited, whereas overexpression of salusin-β enhanced it. These results suggest that salusin-β may induce the translocation of $p47^{phox}$ to the membrane to activate NOX-2 and then trigger the overwhelming formation of ROS and subsequent VC.

In addition, Rac1 is also an important subunit of NAD(P)H oxidase, which is critical for the assembly and activation of NAD(P)H oxidase and the production of ROS (1). In this study, we also found that Rac1 peptide inhibitor W56 remarkably relieved the degree of calcification in calcified medium-incubated VSMCs. Rac1-GTP, the active form of Rac1, was obviously upregulated in calcified VSMCs, which was reduced by salusin-β silencing markedly and further elevated by salusin-β overexpression. These results suggested that Rac1 activation was also involved in the effects of salusin-β on NAD(P)H oxidase activation and ROS production and VSMC calcification.

In the present study, we found that besides NOX-2, the protein levels of both NOX-1 and NOX-4 in calcified VSMCs were also increased time-dependently. Silencing of either NOX-1 or NOX-4 prevented the development of calcification in VSMCs induced by calcified medium, but not the one induced by salusin-β overexpression. In accordance with this, neither salusin-β knockdown nor salusin-β overexpression affected the expressions of NOX-1 and NOX-4 with or without calcification stimulants. These results suggested that although both NOX-1 and NOX-4 genes are player in VSMC calcification, whereas both of which were not required for salusin-β-mediated oxidative stress and VC in VSMCs.

Taken together, these results suggest that salusin-β activates NAD(P)H oxidase-ROS signaling to elicit VSMC calcification. The membrane translocation of $p47^{phox}$, NOX-2 activation, Rac 1 activation, and $p22^{phox}$ are involved in the NAD(P)H oxidase activation mechanism induced by salusin-β. However, NOX-1 and NOX-4 were not necessary in salusin-β-mediated VC.

It is reported that Klotho is modulated by a wide range of triggers, including inflammation, oxidative stress, tumor

necrosis factor, intermedin, rosiglitazone, resveratrol, and angiotensin II (5, 25, 33, 52, 58, 59). Among these, oxidative stress is an important regulator for Klotho gene expression. The association of oxidative stress and Klotho plays a central role in the process of VC (32). H_2O_2 downregulates the expression of Klotho in cultured proximal tubule epithelial cells (29). Soluble Klotho directly protects cells against a variety of affronts, including oxidative stress (35). Klotho has been indicated to decrease oxidative stress to maintain the contractile SMC phenotype and reduce VSMC calcification (32). We explored ROS mediation in the downregulation of Klotho induced by salusin-β-mediated VC. In this study, we found that the downregulation of Klotho induced by calcification medium was rectified by NAC or DPI. Moreover, the direct suppressive effect of salusin-β on Klotho protein was also impeded by NAC and DPI. Thus, we demonstrated that ROS is responsible for Klotho downregulation, contributing to salusin-β-mediated VC. By inference, salusin-β activates NAD(P)H oxidase to produce ROS, which then antagonizes Klotho signaling to boost VSMC calcification. However, we found that the administration of exogenous Klotho prevented the overproduction of superoxide anions, MDA, and H_2O_2 in VSMCs induced by calcified medium or salusin-β overexpression. *In vivo*, the increased NAD(P)H oxidase activity and ROS level of the aortas of rats with salusin-β overexpression were largely ameliorated by chronic application of Klotho. These results suggested that Klotho gene in reverse exhibits antioxidant properties and antagonism effect on salusin-β-induced ROS elevation.

In conclusion, our results highlight the essential role of salusin-β in the osteoblastic differentiation of VSMCs and pathological arterial calcification. The excessive ROS generation and downregulation of Klotho are responsible for salusin-β to facilitate VC and osteochondrogenic transition of VSMCs (A summary flow diagram of mechanisms of salusin-β is shown in Supplementary Fig. S13). However, we cannot exclude the possibility that other mechanisms, such as impaired mitochondrial function (22), increased inflammation response (3), endoplasmic reticulum stress (37), or VSMC apoptosis (42), may account for salusin-β-mediated VC. Future studies will be needed to fully determine the validity of these possibilities. Collectively, targeting the salusin-β/ROS/Klotho pathway may pave the way for the prevention and treatment of VC.

Materials and Methods

Animals and reagents

Experiments were carried out in male Sprague–Dawley rats (Vital River Biological, Beijing, China). Rats were housed under standard temperature and humidity condition on 12:12-h light–dark cycle and given standard rodent chow and water freely. All experiments conformed to the rules and regulations of the Experimental Animal Care and Use Committee of Nanjing Medical University. All procedures were complied with the Guide for the Care and Use of Laboratory Animal published by the U.S. National Institutes of Health (34a). Dulbecco's modified Eagle's medium (DMEM) and fetal bovine serum (FBS) were obtained from Gibco BRL (Carlsbad, CA). Antibodies against Runx2, BMP-2, NOX-1, NOX-2, NOX-4, $p22^{phox}$, $p47^{phox}$, Klotho, and goat anti-rabbit IgG H&L (Alexa Fluor® 488) were purchased from Abcam (Cambridge, MA). Antibodies against salusin-β were purchased from Bachem (Bubendorf, Switzerland). Antibodies against α-SMA, SM22α, CD31, GAPDH, and horseradish peroxidase-conjugated secondary antibodies were purchased from Proteintech Group, Inc. (Wuhan, China). The specific primers and siRNA sequences were synthesized by Sangon Biotech Co., Ltd. (Shanghai, China). Immunohistochemistry kit and diaminobenzidine (DAB) were obtained from Boster Biological Technology Co., Ltd. (Wuhan, China). The recombinant rat Klotho protein was obtained from USCN Business Co., Ltd. (RPH757Ra02, Wuhan, China). DPI, β-GP, and DHE were purchased from Sigma (St. Louis, MO). NAC was obtained from Beyotime Institute of Biotechnology (Shanghai, China). Rac1 peptide inhibitor W56 was procured from TOCRIS Bioscience (Bristol, United Kingdom). Adenoviral constructs carrying shRNA against salusin-β and a control shRNA (a negative control) were constructed by Genomeditech Co. (Shanghai, China) according to our previous reports (49). The NOX-1 shRNA plasmids, NOX-2 shRNA plasmids, NOX-4 shRNA plasmids, $p22^{phox}$ shRNA plasmids, $p47^{phox}$ shRNA plasmids, and control shRNA plasmids, as well as Na^+/K^+ ATPase α1 antibody were purchased from Santa Cruz Biotechnology (Santa Cruz, CA). Recombinant lentivirus vector expressing salusin-β was designed and identified by Invitrogen (Life Tech, Shanghai, China) as previously described (45).

In vivo *rat model of VC*

Sprague–Dawley rats weighing between 180 and 200 g were used to induce VC by application of vitamin D3 plus nicotine as previously described (23). In short, rats were given intramuscular injection with vitamin D3 (300,000 IU/kg) simultaneously with an intragastric dose of nicotine (25 mg/kg in 5 mL peanut oil) at 9:00 a.m. on the first day. Nicotine was given again at 19:00 p.m. on the same day. After 14 days, rats were re-treated with vitamin D3. Rats in the control group received normal saline intramuscularly and two gavages of peanut oil without nicotine (5 mL/kg). For silencing of salusin-β *in vivo*, gene transfer of salusin-β shRNA was performed 3 days after induction of VC. The rats received intravenous injection of phosphate-buffered solution (PBS), adenoviral vectors encoding control shRNA (2.0×10^{10} plaque-forming units), or adenoviral vectors encoding salusin-β shRNA (2.0×10^{10} plaque-forming units) *via* tail vein, respectively. For overexpression of salusin-β *in vivo*, the rats were randomly subjected to injection of PBS, lentivirus vector, or lentivirus expressing salusin-β (1×10^{7} transduction unit) *via* tail vein 3 days after induction of VC. The intravenous injections were repeated 2 weeks after the first administration to ensure the adequate downregulation or upregulation of salusin-β in arteries of rats. After 4 weeks of VC induction, rats were euthanized with a pentobarbital overdose (150 mg/kg, intravenously) to collect plasma for salusin-β level measurement and aortas for calcium deposition assay, von Kossa staining, protein, or RNA extraction. Schematic diagram indicating the timeline of the above experiments in rats is shown in Supplementary Figure S14.

Cell culture and VSMC calcification model

Primary VSMCs were isolated from the thoracic aortic arteries of Sprague–Dawley rats (150–180 g) using enzymatic digestion as previously described (46). VSMCs at

passages 5 to 8 were used for the experiments. VSMCs were cultured in DMEM containing 10% FBS, 100 U/mL penicillin, and 100 mg/mL streptomycin at 37°C in an incubator containing 95% air and 5% CO_2. To induce calcification, confluent VSMCs were incubated in medium containing β-GP (5 m*M*) and Ca^{2+} (2.5 m*M*) for two consecutive weeks as previously described (5). The medium was refreshed once every 2 days. Cells were harvested at the required time points. For silencing of salusin-β *in vitro*, VSMCs were first transfected with adenovirus-mediated shRNA against salusin-β or control shRNA (multiplicity of infection [MOI] = 100) for 48 h and then used to induce calcification. For overexpression of salusin-β *in vitro*, VSMCs were transfected with lentivirus expressing salusin-β or lentiviral vector (MOI = 100) and grown in 5% CO_2 incubator at 37°C for 48 h before administration of β-GP and Ca^{2+} to induce VC.

siRNA or shRNA transfection

For siRNA transfection experiment, the VSMCs were cultured (30%–40% confluent) and transfected for siRNA klotho (klotho siRNA, 100 n*M*, sense, 5′-CCGAAAGUCUU UACUGGCUUUCAUA-3′; antisense, 5′-UAUGAAAGCC AGUAAAGACUUUCGG-3′) and nonsilencing control siRNA (Qiagen, Valencia, CA) by using lipofectamine 2000 transfection reagent (Invitrogen, Carlsbad, CA) according to the manufacturer's recommendations as described previously (62).

For shRNA plasmid transfection experiment, the VSMCs (at 30%–40% confluence) were cultured in antibiotic-free normal growth medium supplemented with FBS. Then, the VSMCs were transfected with negative control shRNA or targeted shRNA (1 μg) using shRNA plasmid transfection reagent (Santa Cruz Biotechnology) following the manufacturer's protocols. The targeted gene-knockdown cells were then treated with calcification medium and subsequently harvested for analysis *via* Western blotting, real-time PCR, and other experiments.

Western blotting

Each sample was lysed in an RIPA buffer with protease inhibitor and phosphatase inhibitor cocktail, and the supernatant was obtained by centrifugation at 4°C. The protein levels of each sample were determined by a modified bicinchoninic acid (BCA) protein assay (Beyotime Biotechnology, Shanghai, China). The samples were separated by sodium dodecyl sulfate–polyacrylamide gel electrophoresis using electrophoresis and blotting apparatus (Bio-Rad) and transferred to nitrocellulose membranes. Blocking was carried out at room temperature with 5% nonfat milk powder prepared in Tris-buffered saline containing 0.1% Tween 20. Then, the membranes were incubated with the primary antibodies at 4°C overnight. Protein loading was normalized by probing all Western blots with GAPDH antibody. The results were quantified using the ImageJ densitometric analysis software (NIH, Bethesda, MD) by comparing the gray value (area multiplied by the mean gray value) between target protein and GAPDH.

Real-time quantitative PCR

Total RNA was extracted from each sample using a Trizol reagent (Life Technologies, Gaithersburg, MD) according to the manufacturer's protocols. RNA concentrations and purity were assessed by the measurement of optical density at 260 and 280 nm. Equal RNA levels (0.5 μg) were reversed transcribed into complementary DNA (cDNA) using HiScriptQ RT SuperMix for quantitative PCR (Vazyme, Nanjing, China). The sequences of primers for salusin-β: 5′-TCACTTCTCTCCTA TCATCCACTCC-3′ (forward); 5′-GGCAGCTTGTCCATCT CATCG-3′ (reverse); Klotho: 5′-ACTTTCTTCTGCCCTAT TTCACG-3′ (forward); 5′-CCAGGTAATCGTTGTATTTTA TCGG-3′ (reverse); GAPDH: 5′-GGAAAGCTGTGGCGTG AT-3′ (forward); 5′-AAGGTGGAAGAATGGGAGTT-3′ (reverse). The expression of targeted mRNA was calculated by subtracting cycle threshold (Ct) values of target genes from Ct values of GAPDH.

Enzyme-linked immunosorbent assay

The levels of salusin-β were quantified using commercially available rat enzyme-linked immunosorbent assay (ELISA) kits (USCN Life Science, Houston, TX) according to the manufacturer's instructions (49). In brief, the standards or sample diluent were added and incubated in the appropriate wells of a precoated ELISA plate. Finally, the optical density was determined using a microplate reader (SYNERGY H4; BioTek).

Immunohistochemistry and immunofluorescence staining

For immunohistochemistry, the rats were perfused through the left ventricle first with 0.01 *M* PBS at pH 7.4 and then with 4% paraformaldehyde. The fixed aortas were dehydrated and embedded in paraffin, then cut into 5-μm sections and mounted on slides. The slides were washed three times with 0.1 *M* PBS after deparaffinization, and then incubated in 3% H_2O_2 for 15 min to quench the endogenous peroxidase. The sections were blocked in 10% goat serum for 60 min at room temperature, followed by incubation with the primary antibody against salusin-β for 24 h at 4°C. The sections were treated with 3,3-DAB to develop the positive cells in arteries. Sections were counterstained with hematoxylin, and the images were captured using a light microscope (Zeiss, Jena, Germany).

For immunohistochemistry, control IgG was used to confirm the specificity of the antibody against salusin-β. As expected, the immunopositive signal was only detected by the antibody against salusin-β, not control IgG or PBS (Supplementary Fig. S15). Stimulated cells were fixed in 4% formaldehyde and permeabilized with 0.1% Triton X-100 in PBS for 15 min. The cells were blocked with 10% goat serum for 30 min and incubated with the primary salusin-β antibody overnight at 4°C. The fixed cells were then incubated with Alexa Fluor 488-conjugated anti-rabbit secondary antibody for 30 min. Nuclei were stained with DAPI. Immunofluorescence signals were visualized on a fluorescence microscope (80i; Nikon).

Detection of ALP activity and calcium content

The ALP assay kit was purchased from Nanjing Jiancheng Bioengineering Institute (Nanjing, China). The ALP activity was measured according to the manufacturer's instructions (60). The absorbance was determined at 520 nm, and the results were normalized to the protein content in each sample. The

content of calcium was measured *via* o-cresolphthalein colorimetric methods as previously described (30). The calcium levels in stimulated cells and aortic samples were normalized to the protein content, as determined by the BCA method (43, 61). ALP activity assays were performed after VSMCs treated with calcifying media for 3 days, and calcium content was measured at the 14th day after β-GP and Ca^{2+} stimulation.

Alizarin Red S staining in cultured VSMCs

The culture medium of cells in 6-well plates was removed, and cells were washed in PBS three times and fixed in 4% neutral formalin for 30 min, followed by incubation with 1% Alizarin Red (1 mL/well) for 30 min. After the staining, cell preparations were washed three times with PBS to eliminate nonspecific staining. The formation of mineralized nodules was captured using a light microscope (Zeiss) (30).

Von Kossa staining

The aorta sections were subjected to von Kossa staining for morphometric assay after deparaffinization and rehydration as previously described (28). The photographs were examined under a light microscope (Zeiss).

Measurement of ROS generation, MDA, H_2O_2, NAD(P)H oxidase activity, and superoxide anions level

The intracellular ROS in VSMCs were determined with fluorescent probe DHE as previously described (48). The collected VSMCs were fixed and incubated in DHE (10 μM) for 30 min in a light-protected humidified chamber. The fluorescence signals were captured and quantified with the IMAGE-PRO PLUS 6.0 (version 6.0; Media Cybernetics, Bethesda, MD). For quantitation detection of oxidative stress markers, the levels of MDA and H_2O_2 were measured by using commercially available assay kits (MDA Assay Kit, TBA method, Item No. A003-1-2; CAT Assay Kit, Visible light method, Item No. A007-1-1; Jiancheng Bioengineering Institute) in accordance with the manufacturer's recommendations as our previous reports (50). NAD(P)H oxidase activity and superoxide anion levels of arteries were measured by enhanced lucigenin-derived chemiluminescence as previously described (36, 47).

Statistical analyses

All data are expressed as mean ± standard error. Statistical analyses were performed using the SPSS 17.0 Statistical Software by IBM (Armonk, NY). Comparisons within two groups were made by Student's *t*-test. Statistical analyses involved one-way analyses of variance for multiple comparisons, then Tukey–Kramer *post hoc* testing. A value of $p < 0.05$ was considered statistically significant.

Authors' Contributions

Y.H. and H.S. designed the research. H.S., F.Z., H.W., and Q.D. performed the research. H.S., S.S., C.G., and Y.X. analyzed the data. H.S., H.T., and Y.H. wrote or contributed to the writing of the article. S.M.B. provided intellectual suggestions and critically reviewed the article.

Author Disclosure Statement

The authors have no conflict of interest to declare.

Funding Information

This work was supported by grants from the Fund of the National Natural Science Foundation of China (81470538, 81700364, 81970052, and 81770059), Qing Lan Project of Jiangsu Province of China, Open Project of State Key Laboratory of Respiratory Disease (SKLRD-OP-201911), Jiangsu Natural Science Foundation (BK20170179), Fundamental Research Funds for the Central Universities (JUSRP11745), project funded by China Postdoctoral Science Foundation (2017M611688), and project funded by Jiangsu Postdoctoral Science Foundation (1701062C).

Supplementary Material

Supplementary Figure S1
Supplementary Figure S2
Supplementary Figure S3
Supplementary Figure S4
Supplementary Figure S5
Supplementary Figure S6
Supplementary Figure S7
Supplementary Figure S8
Supplementary Figure S9
Supplementary Figure S10
Supplementary Figure S11
Supplementary Figure S12
Supplementary Figure S13
Supplementary Figure S14
Supplementary Figure S15
Supplementary Figure S16
Supplementary Figure S17
Supplementary Figure S18
Supplementary Figure S19
Supplementary Figure S20

References

1. Acevedo A and Gonzalez-Billault C. Crosstalk between Rac1-mediated actin regulation and ROS production. *Free Radic Biol Med* 116: 101–113, 2018.
2. Bedard K and Krause KH. The NOX family of ROS-generating NADPH oxidases: physiology and pathophysiology. *Physiol Rev* 87: 245–313, 2007.
3. Bessueille L and Magne D. Inflammation: a culprit for vascular calcification in atherosclerosis and diabetes. *Cell Mol Life Sci* 72: 2475–2489, 2015.
4. Briet M and Burns KD. Chronic kidney disease and vascular remodelling: molecular mechanisms and clinical implications. *Clin Sci (Lond)* 123: 399–416, 2012.
5. Chang JR, Guo J, Wang Y, Hou YL, Lu WW, Zhang JS, Yu YR, Xu MJ, Liu XY, Wang XJ, Guan YF, Zhu Y, Du J, Tang CS, and Qi YF. Intermedin1-53 attenuates vascular calcification in rats with chronic kidney disease by upregulation of alpha-Klotho. *Kidney Int* 89: 586–600, 2016.
6. Chistiakov DA and Myasoedova VA. Calcifying matrix vesicles and atherosclerosis. *Biomed Res Int* 2017: 7463590, 2017.

7. Duan XH, Chang JR, Zhang J, Zhang BH, Li YL, Teng X, Zhu Y, Du J, Tang CS, and Qi YF. Activating transcription factor 4 is involved in endoplasmic reticulum stress-mediated apoptosis contributing to vascular calcification. *Apoptosis* 18: 1132–1144, 2013.
8. Fujimoto K, Hayashi A, Kamata Y, Ogawa A, Watanabe T, Ichikawa R, Iso Y, Koba S, Kobayashi Y, Koyama T, and Shichiri M. Circulating levels of human salusin-beta, a potent hemodynamic and atherogenesis regulator. *PLoS One* 8: e76714, 2013.
9. Geiszt M. NADPH oxidases: new kids on the block. *Cardiovasc Res* 71: 289–299, 2006.
10. Giacco F, Brownlee M. Oxidative stress and diabetic complications. *Circ Res* 107: 1058–1070, 2010.
11. Guo Y, Zhuang X, Huang Z, Zou J, Yang D, Hu X, Du Z, Wang L, and Liao X. Klotho protects the heart from hyperglycemia-induced injury by inactivating ROS and NF-kappaB-mediated inflammation both in vitro and in vivo. *Biochim Biophys Acta Mol Basis Dis* 1864: 238–251, 2018.
12. Hawkins CL. Protein carbamylation: a key driver of vascular calcification during chronic kidney disease. *Kidney Int* 94: 12–14, 2018.
13. Hilenski LL, Clempus RE, Quinn MT, Lambeth JD, and Griendling KK. Distinct subcellular localizations of Nox1 and Nox4 in vascular smooth muscle cells. *Arterioscler Thromb Vasc Biol* 24: 677–683, 2004.
14. Ho E, Karimi Galougahi K, Liu CC, Bhindi R, and Figtree GA. Biological markers of oxidative stress: applications to cardiovascular research and practice. *Redox Biol* 1: 483–491, 2013.
15. Hu MC, Kuro-o M, and Moe OW. alphaKlotho and vascular calcification: an evolving paradigm. *Curr Opin Nephrol Hypertens* 23: 331–339, 2014.
16. Hu MC, Shi M, Zhang J, Quinones H, Griffith C, Kuro-o M, and Moe OW. Klotho deficiency causes vascular calcification in chronic kidney disease. *J Am Soc Nephrol* 22: 124–136, 2011.
17. Jia G, Aroor AR, Jia C, and Sowers JR. Endothelial cell senescence in aging-related vascular dysfunction. *Biochim Biophys Acta Mol Basis Dis* 1865: 1802–1809, 2019.
18. Johnson RC, Leopold JA, and Loscalzo J. Vascular calcification: pathobiological mechanisms and clinical implications. *Circ Res* 99: 1044–1059, 2006.
19. Kapustin AN, and Shanahan CM. Emerging roles for vascular smooth muscle cell exosomes in calcification and coagulation. *J Physiol* 594: 2905–2914, 2016.
20. Kay AM and Simpson CL. The role of AGE/RAGE signaling in diabetes-mediated vascular calcification. *J Diabetes Res* 2016: 6809703, 2016.
21. Lassegue B, Sorescu D, Szocs K, Yin Q, Akers M, Zhang Y, Grant SL, Lambeth JD, and Griendling KK. Novel gp91(phox) homologues in vascular smooth muscle cells: nox1 mediates angiotensin II-induced superoxide formation and redox-sensitive signaling pathways. *Circ Res* 88: 888–894, 2001.
22. Leem J and Lee IK. Mechanisms of vascular calcification: the pivotal role of pyruvate dehydrogenase kinase 4. *Endocrinol Metab (Seoul)* 31: 52–61, 2016.
23. Li H, Teng X, Yang R, Guo Q, Xue H, Xiao L, Duan X, Tian D, Feng X, and Wu Y. Hydrogen sulfide facilitates the impaired sensitivity of carotid sinus baroreflex in rats with vascular calcification. *Front Pharmacol* 8: 629, 2017.
24. Lim K, Lu TS, Molostvov G, Lee C, Lam FT, Zehnder D, and Hsiao LL. Vascular Klotho deficiency potentiates the development of human artery calcification and mediates resistance to fibroblast growth factor 23. *Circulation* 125: 2243–2255, 2012.
25. Liu L, Liu Y, Zhang Y, Bi X, Nie L, Liu C, Xiong J, He T, Xu X, Yu Y, Yang K, Gu J, Huang Y, Zhang J, Zhang Z, Zhang B, and Zhao J. High phosphate-induced downregulation of PPARgamma contributes to CKD-associated vascular calcification. *J Mol Cell Cardiol* 114: 264–275, 2018.
26. Liu QF, Ye JM, Yu LX, Dong XH, Feng JH, Xiong Y, Gu XX, and Li SS. Klotho mitigates cyclosporine A (CsA)-induced epithelial-mesenchymal transition (EMT) and renal fibrosis in rats. *Int Urol Nephrol* 49: 345–352, 2017.
27. Liu Y, Lin F, Fu Y, Chen W, Liu W, Chi J, Zhang X, and Yin X. Cortistatin inhibits arterial calcification in rats via GSK3beta/beta-catenin and protein kinase C signalling but not c-Jun N-terminal kinase signalling. *Acta Physiol (Oxf)* 223: e13055, 2018.
28. Liu Y, Zhou YB, Zhang GG, Cai Y, Duan XH, Teng X, Song JQ, Shi Y, Tang CS, Yin XH, and Qi YF. Cortistatin attenuates vascular calcification in rats. *Regul Pept* 159: 35–43, 2010.
29. Liu YN and Zhou J. Sulodexide protects renal tubular epithelial cells from oxidative stress-induced injury via upregulating klotho expression at an early stage of diabetic kidney disease. *J Diabetes Res* 2017: 4989847, 2017.
30. Ma YY, Sun L, Chen XJ, Wang N, Yi PF, Song M, Zhang B, Wang YZ, and Liang QH. Vinpocetine attenuates the osteoblastic differentiation of vascular smooth muscle cells. *PLoS One* 11: e0162295, 2016.
31. Mazzini MJ and Schulze PC. Proatherogenic pathways leading to vascular calcification. *Eur J Radiol* 57: 384–389, 2006.
32. Mencke R and Hillebrands JL. The role of the anti-ageing protein klotho in vascular physiology and pathophysiology. *Ageing Res Rev* 35: 124–146, 2017.
33. Mitobe M, Yoshida T, Sugiura H, Shirota S, Tsuchiya K, and Nihei H. Oxidative stress decreases klotho expression in a mouse kidney cell line. *Nephron Exp Nephrol* 101: e67–e74, 2005.
34. Nagashima M, Watanabe T, Shiraishi Y, Morita R, Terasaki M, Arita S, Hongo S, Sato K, Shichiri M, Miyazaki A, and Hirano T. Chronic infusion of salusin-alpha and -beta exerts opposite effects on atherosclerotic lesion development in apolipoprotein E-deficient mice. *Atherosclerosis* 212: 70–77, 2010.

34a. National Research Council; Division on Earth and Life Studies; Institute for Laboratory Animal Research; Committee for the Update of the Guide for the Care and Use of Laboratory Animals. Guide for the Care and Use of Laboratory Animals. Washington, DC: The National Academies Press, 2011, p. 246.

35. Ravikumar P, Ye J, Zhang J, Pinch SN, Hu MC, Kuro-o M, Hsia CC, and Moe OW. alpha-Klotho protects against oxidative damage in pulmonary epithelia. *Am J Physiol Lung Cell Mol Physiol* 307: L566–L575, 2014.
36. Ren XS, Ling L, Zhou B, Han Y, Zhou YB, Chen Q, Li YH, Kang YM, and Zhu GQ. Silencing salusin-beta attenuates cardiovascular remodeling and hypertension in spontaneously hypertensive rats. *Sci Rep* 7: 43259, 2017.
37. Rogers MA and Aikawa E. Cardiovascular calcification: artificial intelligence and big data accelerate mechanistic discovery. *Nat Rev Cardiol* 16: 261–274, 2019.

38. Shanahan CM. Inflammation ushers in calcification: a cycle of damage and protection? *Circulation* 116: 2782–2785, 2007.
39. Shao JS, Cai J, and Towler DA. Molecular mechanisms of vascular calcification: lessons learned from the aorta. *Arterioscler Thromb Vasc Biol* 26: 1423–1430, 2006.
40. Shichiri M, Ishimaru S, Ota T, Nishikawa T, Isogai T, and Hirata Y. Salusins: newly identified bioactive peptides with hemodynamic and mitogenic activities. *Nat Med* 9: 1166–1172, 2003.
41. Shimamura Y, Hamada K, Inoue K, Ogata K, Ishihara M, Kagawa T, Inoue M, Fujimoto S, Ikebe M, Yuasa K, Yamanaka S, Sugiura T, and Terada Y. Serum levels of soluble secreted alpha-klotho are decreased in the early stages of chronic kidney disease, making it a probable novel biomarker for early diagnosis. *Clin Exp Nephrol* 16: 722–729, 2012.
42. Shioi A. Vascular calcification—pathological mechanism and clinical application—mechanisms of vascular calcification [in Japanese]. *Clin Calcium* 25: 635–643, 2015.
43. Sun H, Zhu X, Lin W, Zhou Y, Cai W, and Qiu L. Interactions of TLR4 and PPARgamma, dependent on AMPK signalling pathway contribute to anti-inflammatory effects of vaccariae hypaphorine in endothelial cells. *Cell Physiol Biochem* 42: 1227–1239, 2017.
44. Sun HJ, Chen D, Wang PY, Wan MY, Zhang CX, Zhang ZX, Lin W, and Zhang F. Salusin-beta is involved in diabetes mellitus-induced endothelial dysfunction via degradation of peroxisome proliferator-activated receptor gamma. *Oxid Med Cell Longev* 2017: 6905217, 2017.
45. Sun HJ, Liu TY, Zhang F, Xiong XQ, Wang JJ, Chen Q, Li YH, Kang YM, Zhou YB, Han Y, Gao XY, and Zhu GQ. Salusin-beta contributes to vascular remodeling associated with hypertension via promoting vascular smooth muscle cell proliferation and vascular fibrosis. *Biochim Biophys Acta* 1852: 1709–1718, 2015.
46. Sun HJ, Ren XS, Xiong XQ, Chen YZ, Zhao MX, Wang JJ, Zhou YB, Han Y, Chen Q, Li YH, Kang YM, and Zhu GQ. NLRP3 inflammasome activation contributes to VSMC phenotypic transformation and proliferation in hypertension. *Cell Death Dis* 8: e3074, 2017.
47. Sun HJ, Zhang LL, Fan ZD, Chen D, Zhang L, Gao XY, Kang YM, and Zhu GQ. Superoxide anions involved in sympathoexcitation and pressor effects of salusin-beta in paraventricular nucleus in hypertensive rats. *Acta Physiol (Oxf)* 210: 534–545, 2014.
48. Sun HJ, Zhao MX, Liu TY, Ren XS, Chen Q, Li YH, Kang YM, and Zhu GQ. Salusin-beta induces foam cell formation and monocyte adhesion in human vascular smooth muscle cells via miR155/NOX2/NFkappaB pathway. *Sci Rep* 6: 23596, 2016.
49. Sun HJ, Zhao MX, Ren XS, Liu TY, Chen Q, Li YH, Kang YM, Wang JJ, and Zhu GQ. Salusin-beta promotes vascular smooth muscle cell migration and intimal hyperplasia after vascular injury via ROS/NFkappaB/MMP-9 pathway. *Antioxid Redox Signal* 24: 1045–1057, 2016.
50. Sun HJ, Zhou H, Feng XM, Gao Q, Ding L, Tang CS, Zhu GQ, and Zhou YB. Superoxide anions in the paraventricular nucleus mediate cardiac sympathetic afferent reflex in insulin resistance rats. *Acta Physiol (Oxf)* 212: 267–282, 2014.
51. Ter Braake AD, Shanahan CM, and de Baaij JHF. Magnesium counteracts vascular calcification: passive interference or active modulation? *Arterioscler Thromb Vasc Biol* 37: 1431–1445, 2017.
52. Thurston RD, Larmonier CB, Majewski PM, Ramalingam R, Midura-Kiela M, Laubitz D, Vandewalle A, Besselsen DG, Muhlbauer M, Jobin C, Kiela PR, and Ghishan FK. Tumor necrosis factor and interferon-gamma downregulate klotho in mice with colitis. *Gastroenterology* 138: 1384–1394, 1394.e1–1394.e2, 2010.
53. Towler DA and Demer LL. Thematic series on the pathobiology of vascular calcification: an introduction. *Circ Res* 108: 1378–1380, 2011.
54. van der Zee S, Baber U, Elmariah S, Winston J, and Fuster V. Cardiovascular risk factors in patients with chronic kidney disease. *Nat Rev Cardiol* 6: 580–589, 2009.
55. Watanabe T, Nishio K, Kanome T, Matsuyama TA, Koba S, Sakai T, Sato K, Hongo S, Nose K, Ota H, Kobayashi Y, Katagiri T, Shichiri M, and Miyazaki A. Impact of salusin-alpha and -beta on human macrophage foam cell formation and coronary atherosclerosis. *Circulation* 117: 638–648, 2008.
56. Winiarska K, Dzik JM, Labudda M, Focht D, Sierakowski B, Owczarek A, Komorowski L, and Bielecki W. Melatonin nephroprotective action in Zucker diabetic fatty rats involves its inhibitory effect on NADPH oxidase. *J Pineal Res* 60: 109–117, 2016.
57. Yang Y, Sun Y, Chen J, Bradley WE, Dell'Italia LJ, Wu H, and Chen Y. AKT-independent activation of p38 MAP kinase promotes vascular calcification. *Redox Biol* 16: 97–103, 2018.
58. Yoon HE, Ghee JY, Piao S, Song JH, Han DH, Kim S, Ohashi N, Kobori H, Kuro-o M, and Yang CW. Angiotensin II blockade upregulates the expression of Klotho, the anti-ageing gene, in an experimental model of chronic cyclosporine nephropathy. *Nephrol Dial Transplant* 26: 800–813, 2011.
59. Zhang P, Li Y, Du Y, Li G, Wang L, and Zhou F. Resveratrol ameliorated vascular calcification by regulating Sirt-1 and Nrf2. *Transplant Proc* 48: 3378–3386, 2016.
60. Zhou YB, Gao Q, Li P, Han Y, Zhang F, Qi YF, Tang CS, Gao XY, and Zhu GQ. Adrenomedullin attenuates vascular calcification in fructose-induced insulin resistance rats. *Acta Physiol (Oxf)* 207: 437–446, 2013.
61. Zhu X, Zhou Z, Zhang Q, Cai W, Zhou Y, Sun H, and Qiu L. Vaccarin administration ameliorates hypertension and cardiovascular remodeling in renovascular hypertensive rats. *J Cell Biochem* 119: 926–937, 2018.
62. Zhu Y, Takayama T, Wang B, Kent A, Zhang M, Binder BY, Urabe G, Shi Y, DiRenzo D, Goel SA, Zhou Y, Little C, Roenneburg DA, Shi XD, Li L, Murphy WL, Kent KC, Ke J, and Guo LW. Restenosis inhibition and re-differentiation of TGFbeta/Smad3-activated smooth muscle cells by resveratrol. *Sci Rep* 7: 41916, 2017.

Address correspondence to:
Dr. Ying Han
Key Laboratory of Targeted Intervention of Cardiovascular Disease
Collaborative Innovation Center of Translational Medicine for Cardiovascular Disease
Department of Physiology
Nanjing Medical University
Nanjing
Jiangsu 211166
China

E-mail: yhancn@njmu.edu.cn

Prof. Haiyang Tang
State Key Laboratory of Respiratory Disease
National Clinical Research Center for Respiratory Disease
Guangzhou Institute of Respiratory Health
The First Affiliated Hospital of Guangzhou
Medical University
Guangzhou
Guangdong 510120
China

E-mail: tanghy2008@yahoo.com

Date of first submission to ARS Central, January 5, 2019; date of final revised submission, September 16, 2019; date of acceptance, October 1, 2019.

Abbreviations Used

α-SMA = alpha smooth muscle actin
β-GP = β-glycerophosphate
ALP = alkaline phosphatase
BMP = bone morphogenetic protein
Ct = cycle threshold
DAB = diaminobenzidine
DHE = dihydroethidium
DMEM = Dulbecco's modified Eagle's medium
DPI = diphenyleneiodonium chloride
ELISA = enzyme-linked immunosorbent assay
FBS = fetal bovine serum
H_2O_2 = hydrogen peroxide
MDA = malondialdehyde
mRNA = messenger RNA
NAC = N-acetyl-L-cysteine
NAD(P)H = nicotinamide adenine dinucleotide phosphate
NIH = National Institutes of Health
NOX = NAD(P)H oxidase
PCR = polymerase chain reaction
PBS = phosphate-buffered solution
Rac1 = Ras-related C3 botulinum toxin substrate 1
ROS = reactive oxygen species
Runx2 = runt-related transcription factor 2
shRNA = small hairpin RNA
siRNA = small interfering RNA
SM22α = smooth muscle 22 alpha
VC = vascular calcification
VSMCs = vascular smooth muscle cells